Astron. Astrophys. 351, 841–859 (1999)

ASTRONOMY AND ASTROPHYSICS

Comparison of the redshift evolution of dLy α absorbers with predictions from models for the viscous evolution of the Galactic disk

H. Meusinger and R. Thon

Thüringer Landessternwarte Tautenburg, Sternwarte 5, 07778 Tautenburg, Germany

Received 28 January 1999 / Accepted 14 September 1999

Abstract. We analyse predictions for high-z damped Lyman α (dLyα) QSO absorber systems from a special type of disk galaxy evolution models. The models include secular gas infall onto the disk and viscous radial gas flows within the disk. In a previous study, we have shown that these models provide a reasonable fit for all relevant observational properties of the Galactic disk. We discuss the evolution with redshift of the frequency distribution of the H I column density, the metallicity, and the star formation rate. The model predictions are compared with observational data from dLyα QSO absorbers on the assumption that these absorber systems represent early evolutionary stages of present-day spiral galaxies. We study two groups of models with different infall histories. Slow disk evolution models with strong gas infall are in poor agreement with all observational constraints. Moderate infall models provide a better agreement.

Although some of the observed properties of dLyα systems are well reproduced by the models, there remain serious discrepancies. We confirm earlier findings that the model predictions for observed properties of the absorber systems strongly depend on the rôle of dust at high redshift. We apply Monte Carlo simulations to take into account a bias against high column density/high metallicity systems due to extinction of the QSO light by dust in the absorber galaxy. The results of the simulations provide an improved fit of the observed redshift-metallicity relation after the bias is taken into account. However, the predicted abundance scatter for models of the Galactic disks appears too small at intermediate and low redshifts. Furthermore, a deficiency of high column density systems would be expected for $z \lesssim 1.5$ due to the extinction bias. A better agreement with observations is expected if dLyα systems are associated with various galaxy types. The observed HI column density distribution at low redshift must obviously be explained by the contribution of galaxies having high HI column densities but low metallicities. The observed abundance ratio of alpha elements to iron peak elements seems to be nearly solar after correction for dust depletion, whereas the models clearly predict an overabundance of alpha elements at high redshift. The models predict too a high number density of absorber galaxies at $z = 0$ when the distribution of absorbers at high redshift is matched. We discuss possible solutions for these discrepancies.

Correspondence to: meus@tls-tautenburg.de

Key words: ISM: abundances – ISM: dust, extinction – Galaxy: evolution – galaxies: evolution – galaxies: quasars: absorption lines

1. Introduction

Over the last years, our picture of galaxy evolution at intermediate and high redshift has achieved a spectacular evolution (e.g., D'Odorico et al. 1998). The connection between normal galaxies in the local Universe and high-redshift absorber systems in QSO spectra is of particular interest. QSO absorption lines have been considered an important diagnostic tool for studying the evolution of matter at large look-back times for many years (Weymann et al. 1981; Blades et al. 1988). Absorption systems with damped Lyman α (dLyα) lines have attracted particular attention because they were found to be the best candidates for high-redshift progenitors of the disks of present-day spiral galaxies (Wolfe et al. 1986; Wolfe 1988, 1995). This believe is essentially based on the following arguments: *(1.)* Damped Lyα absorption systems have neutral hydrogen column densities of $N(\mathrm{H\,I}) = 2\,10^{20}...10^{22}\,\mathrm{cm}^{-2}$, comparable to what is seen in stars in present-day spiral galaxies. At high redshift, most of the neutral gas in the Universe arises in dLyα systems. The mass density of baryons in these systems is thought to be the same as the mass density contained in present-day spiral galaxies (Lanzetta et al. 1995; Wolfe et al. 1995; Storrie-Lombardi et al. 1996). At lowest redshift, the comoving mass density in dLyα systems is of the same order of magnitude as the global H I density derived from 21 cm studies of nearby spirals (Rao & Briggs 1993; Fall & Pei 1993). *(2.)* The distribution of dLyα column densities evolves with redshift in a characteristic manner where the frequency of high density absorbers decreases faster with decreasing redshift than the frequency of occurence of lower density absorption. It seems tempting to interpret such evolution as due to gas consumption by galactic star formation (Lanzetta et al. 1995; Wolfe et al. 1995; Malaney & Chaboyer 1996). *(3.)* The presence of heavy chemical elements indicates that star formation has taken place. The typical metallicity of about one tenth solar approximately corresponds to what is expected for early phases of galaxy evolution (Timmes et al. 1995a; Wolfe & Prochaska 1998). The slow evolution of metallicity with redshift

(Pettini et al. 1997; Boissé et al. 1998) may be taken as indicative for a slow process of star formation as is expected for disks of spiral galaxies (e.g., Kennicutt 1998). *(4.)* The physical conditions (ionisation state, rotation velocity) in dLyα systems are similar to those for the interstellar medium in large disk galaxies (Wolfe 1995; Prochaska & Wolfe 1997; Michalitsianos et al. 1997; Jedamzik & Prochaska 1998), though there are also opposite claims (Haehnelt et al. 1998; Ledoux et al. 1998).

It still remains a matter of debate whether these arguments are stringent enough to convince of the assumption that the majority of dLyα absorption arises in large, young disks. In the local Universe, the high-mass range of the H I mass function seems to be dominated by spiral galaxies (Zwaan et al. 1997). The picture is much less clear at high redshift. So far, direct imaging revealed a weak association of Lyα absorption systems with galaxies detected in emission at the same z (Le Brun & Bergeron 1998). For absorbers of lower H I column densities the amount of gas along the line of sight is related to the impact parameter of optical galaxies (Chen et al. 1998). Direct imaging studies of fields around QSOs with damped Lyα absorption lines revealed a large number of probably associated galaxies (Aragón-Salamanca et al. 1996; Le Brun et al. 1997; Lanzetta et al. 1997; Mannucci et al. 1998). In several cases, the most likely candidates resemble normal present-day spiral galaxies (e.g., Pettini et al. 1999b), but other types are also present. In particular, it can not be excluded that dLyα absorption at high z is associated with galaxy building blocks resembling dwarf galaxies (Tyson 1988; York 1988; Matteucci et al. 1997; Pettini et al. 1997; Haehnelt et al. 1998). Lyα emission could not be unambiguously identified for most dLyα absorption systems, perhaps simply because Lyα photons are not the ideal tracer for bursts of star formation (see Pettini et al. 1995b). Lyman α emission has been measured for the dLyα absorbers towards the QSOs Q 01151+048, $z_{abs} = 2.81$ (Møller et al. 1998; Fynbo et al. 1999), PKS 0528-250, $z_{abs} = 3.15$ (Møller & Warren 1993), Q 2059-360, $z_{abs} = 3.08$ (Pettini et al. 1995b, Leibundgut & Robertson 1998), and Q 2233+131, $z_{abs} = 3.15$ (Djorgovski et al. 1996). For the first three of these systems, the absorption redshift is very close to the QSO emission redshift. Møller et al. (1998) suggested that the Lyα emission for the absorbers towards Q 0151+048 and Q 2059-360 may be due to photoionisation by the QSOs. The properties derived by Djorgovski et al. for the Lyα emission system related to the dLyα towards Q 2233+131 correspond to those expected of a young disk galaxy. On the other hand, Le Brun et al. (1997) found a wide range of morphological types for optical galaxies near the sightlines to seven QSOs with intermediate redshift absorption systems.

In the present paper, we start with the assumption – as a working hypothesis – that dLyα systems trace the early evolution of present-day spirals of the type of our Galaxy. If this is true, it is tempting to confront galaxy evolution models with the most relevant observational properties of these objects, namely the column density evolution and chemical element abundances evolution. Prochaska & Wolfe (1997) emphasize that relations and conditions deduced from dLyα systems "should tell us more about the history of galaxies at large redshifts than analogous relations deduced from old stars found in the solar neighborhood".

First evolution models of dLyα systems have been discussed by Lanzetta et al. (1995) and Wolfe et al. (1995). They applied a simple closed-box galaxy evolution model, essentially based on a Schmidt-type law for the star formation rate, and were able to reproduce the gas column density evolution of dLyα systems. The price for the simplicity of the model was a "cosmic G dwarf problem". However, the simple closed-box model is, despite its heuristic value, not a realistic description for the evolution of our Galaxy. Kauffmann (1996) has studied the predictions for the gas properties of high-redshift galaxies from models of hierarchical galaxy formation. She could show that such models reproduce not only many of the observed properties of typical present-day spiral galaxies, but also the evolution with redshift of the dLyα column density distribution.

In the present paper, we discuss a different type of galaxy evolution models in the context of gas density and chemical evolution of dLyα absorbers. The essentials of these models are long-term gas accretion onto the disk and viscous radial gas flows within the disk. Both infall models and viscous gas flow models of Galactic evolution have been the subject of many detailed studies. In paper 1 (Thon & Meusinger 1998) we have investigated hybrid (infall+viscosity) models, and we were able to reproduce a large set of observational constraints from the Galactic disk. Viscous evolution of gaseous disks is expected to have a considerable effect on the evolution of the distribution of gas column densities at high redshift (Olivier et al. 1991). The main aim of the present study is to make inferences about the evolution at high redshift of both the gas density and the metallicity and to compare the model predictions with observations from dLyα systems.

One of the shortcomings of the models from paper 1 is their unability to produce strong radial abundance gradients. Although the predicted gradients still fall within the range of the uncertainties of the observational data for the Galactic disk, it is important to study the consequences of differently strong model abundance gradients for the predicted metallicity evolution of dLyα absorbers, especially for the metallicity scatter. For the present study, we add therefore to the models from paper 1 a slightly different viscous disk evolution model (Meusinger & Thon, in preparation) which is able to produce stronger radial abundance gradients.

The interpretation of the observational properties of dLyα systems strongly depends on the rôle of dust at high redshift (Fall & Pei 1993; Pei & Fall 1995; Boissé et al. 1998). Given the low dust-to-gas ratio derived from the known systems (Pei et al. 1991; Lu et al. 1996; Vladilo 1998), one may argue that the effects of extinctions are small. Although this conclusion is not necessarily true (Boissé et al. 1998), we start with neglecting the effect of dust. However, we will take into account depletion into dust grains in the context of metallicity evolution. In a second step, we will try to simulate the selection bias in the observational data due to dust extinction.

We start with a summary of the properties of the models in Sect. 2, followed by a brief discussion of the star formation rate (SFR) history (Sect. 3). In Sect. 4, we use the gas column density evolution from the models to compute the frequency distribution of dLyα absorber column densities. Sect. 5 deals with aspects of chemical evolution at high redshift, and in Sect. 6 we present the modification of the results after the dust extinction bias is taken into account. Finally, the results are briefly discussed in Sect. 7, followed by the conclusions in Sect. 8.

2. The galaxy evolution models

The galaxy evolution models have been described in detail in paper 1. Here, we give a brief summary of the essential ideas and general properties.

- The evolution starts with an initial disk which is assumed to be formed during the self-similar contraction of the baryonic matter in an initial isothermal sphere of a mixture of baryons and dark matter (see Olivier et al. 1991). The radial density profile of the initial disk is that of a truncated isothermal sphere with a large ratio of core radius to truncation radius $r_c/r_t \approx 0.4$ (Blumenthal et al. 1986; Yoshii & Sommer-Larsen 1989; Sommer-Larsen & Yoshii 1989; Sommer-Larsen & Yoshii 1990; Olivier et al. 1991). Alternatively, models starting with a more centrally concentrated mass distribution, i.e. $r_c/r_t \approx 0.1$, were considered, too.
- Disk evolution is strongly affected by secular gas infall. Such secular infall has been suggested to be an important aspect in Galactic evolution by many studies (e.g., Larson 1972; Lynden-Bell 1975; Pagel & Patchett 1975; Prantzos & Aubert 1995; Pilyugin & Edmunds 1997; van den Hoek & de Jong 1997) and finds a natural explanation in the context of hierarchical clustering theory (White & Rees 1978; Kauffmann 1996; Mo et al. 1998). Gas infall is assumed to be a continuous process, though discrete accretion does not significantly alter the model results. The infall rate I and infall timescale t_i are simple, parametrized function of time and galactocentric radius R with $t_i(R) \propto R$, where $t_i(R_\odot)$ is varied between about $0.5\,t_1$ and $2\,t_1$ ($t_1 = 12$ Gyr is the present age of the disk). Total mass fractions $i = 0.5$ and 0.95, respectively, were adopted for the infalling material.
- Following the suggestions by Silk & Norman (1981) and Pringle (1981) on the possible importance of viscous mechanisms in the disk evolution, our models include radial gas flows within the disk due to viscosity in the interstellar medium. The treatment of viscous evolution widely follows the standard approaches (Lin & Pringle 1987a,b; Clarke 1989; Sommer-Larsen & Yoshii 1998, 1990; Olivier et al. 1991; Tsujimoto et al. 1995). The most fundamental assumption of the models is that viscosity and star formation are linked to the same processes so that the timescale of viscous gas transport is similar to the timescale of gas consumption by star formation (Lin-Pringle assumption; Lin & Pringle 1987a), i.e.

$$\beta \equiv t_*/t_\nu \approx 1. \quad (1)$$

In paper 1, we have adopted the viscosity desription from Lin & Pringle (1987b), $\nu = \nu_0 \Sigma_g^a R^b$, which yields, in combination with Eq. (1), the SFR:

$$\Psi = \frac{\nu_0}{\beta} \Sigma_g^{a+1} R^{b-2}, \quad (2)$$

where Σ_g is the gas column density and ν_0, a, b are free parameters for the viscosity. We call models of this type ΣR-models.

A different type of models starts with a description of the SFR and applies the Lin-Pringle assumption to compute the viscosity. In these models, star formation in galaxy disks is assumed to be driven by the local gravitational instability of the gaseous disk, described by Toomre's instability parameter Q. Following Wang & Silk (1994), we assume that the inverse of the star formation timescale is intimately related to the growth rate of the gravitational instability. This yields the SFR in terms of Q

$$\Psi = \epsilon \kappa \Sigma_g \frac{\sqrt{1-Q^2}}{Q}, \quad (3)$$

where ϵ is the efficiency of star formation, κ is the epicyclic frequency, and Q is the instability parameter of a thin disk with a mixture of gas and stars. In the following, models of this type are called Q-models. With regard to the observed properties of the Galactic disk, the Q-models are, in general, quite similar to the ΣR-models. One remarkable exception is the fact that Q-models are able to produce stronger radial abundance gradients. A full description of the Q-models is in preparation.

- Viscosity-induced radial gas flows are particularly strong during the initial evolution of the disk. In the inner disk, the viscous flows concentrate the gas strongly toward the center. The outer disk is spreading due to outward directed flows. The Lin-Pringle assumption leads to a quick formation of an exponential stellar density profile over several scalelengths in agreement with the observed exponential density profiles. The strong, overexponential central stellar mass concentration generally predicted by these models can eventually be related to galactic bulges (cf. also Tsujimoto et al. 1995; Courthau et al. 1996).
- Chemical element abundances are computed as a function of R and t for iron and oxygen. The oxygen enrichment is dominated by supernovae of type II (SN II), while supernovae of type Ia (SN Ia) significantly contribute to the iron enrichment. The modelling of the chemical enrichment due to SN Ia follows the formulation by Greggio & Renzini (1983) and Matteucci & Greggio (1986) for degenerated white dwarfs in symbiotic binaries as progenitors. The initial mass function and the frequency distribution of the mass ratio in SN Ia progenitor binaries are taken from solar neighbourhood data (Kroupa et al. 1993; Duquennoy & Mayor 1991).

There are several free model parameters: the Lin-Pringle parameter β, the mass fraction i and the timescales $t_i(R_\odot)$ of

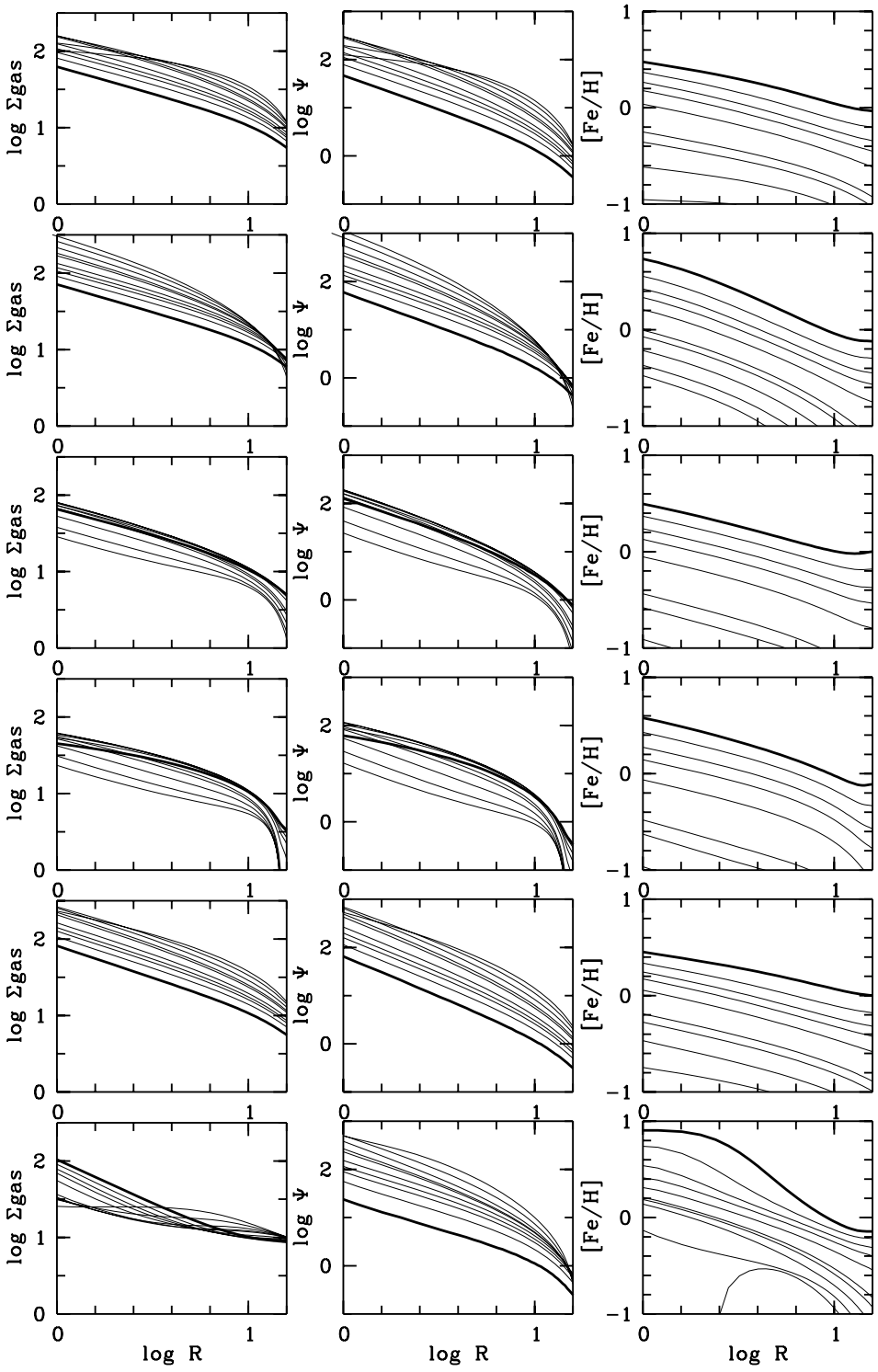

Fig. 1. Evolution of radial profiles of gas density (left), SFR (middle), and [Fe/H] (right) for the models 1 to 6 from Table 1 (from top to bottom). The curves correspond to 10 timesteps (0.24, 0.36, 0.60, 0.96, 1.2, 2.4, 3.6, 4.8, 7.2, 12.0 Gyr) with the thick curve for 12 Gyr. (R in kpc, Σ_g in $m_\odot$ pc^{-2}, Ψ in $m_\odot$ pc^{-2} Gyr^{-1}).

gas infall, the fraction A of binaries evolving to SN Ia, and the total (baryonic) mass of the resulting disk. Furthermore, in ΣR-models, we have the parameters a, b, and ν_0 for the viscosity, while in the Q-models the star formation efficiency ϵ and the velocity dispersion of the gas are free parameters. Realistic models of the Galactic disk were selected by the confrontation with a large set of observational constraints within the framework of an extended parameter study followed by a detailed search for best-fit models. Some of the ΣR-models providing a reasonable match to the observations were discussed in paper 1.

In the context of the present paper, we will discuss six different models. The model parameters and resulting properties are listed in Table 1. Models 1 to 5 are variants of the ΣR-model with $(a, b) = (1, 2)$, corresponding to a quadratic Schmidt-law

Table 1. Parameters of 6 models for the evolution of the Galactic disk. The horizontal line separates input parameters (top) from results (bottom).

model	1	2	3	4	5	6
type	ΣR	ΣR	ΣR	ΣR	ΣR	Q
β	0.5	0.5	0.5	0.18	1.0	0.5
$(a, b, v_g)^*$	(1,2,–)	(1,2,–)	(1,2,–)	(1,2,–)	(1,2,–)	(–,–,7)
$(\nu_0, \epsilon)^*$	(0.0060,–)	(0.0060,–)	(0.015,–)	(0.0055,–)	(0.01,–)	(–,0.003)
$(i, t_i(R_\odot))$	(0.5,6.4)	(0.5,6.4)	(0.95,25.6)	(0.95,25.6)	(0.5,6.4)	(0.5,6.4)
$m_{tot,1}$	$6.3\,10^{10}$	$7.5\,10^{10}$	$6.3\,10^{10}$	$5.0\,10^{10}$	$8.4\,10^{10}$	$6.3\,10^{10}$
A	0.16	0.16	0.30	0.25	0.20	0.35
remark	-	$r_c/r_t \approx 0.1$	-	$v_\phi^{inf}/v_\phi = 0.8$	-	-
$m_{d,1}(R > 15)$	$1.2\,10^{10}$	$1.1\,10^{10}$	$1.0\,10^{10}$	$3.4\,10^{9}$	$1.1\,10^{10}$	$1.8\,10^{10}$
$m_{b,1}$	$1.0\,10^{10}$	$1.8\,10^{10}$	$1.2\,10^{10}$	$4.3\,10^{9}$	$1.8\,10^{10}$	$1.0\,10^{10}$
$l_*(R_\odot, t_1)$	3.9	3.5	3.6	3.4	3.6	3.8
$l_g(R_\odot, t_1)$	8.5	8.5	7.5	7.2	7.9	9
$\Psi(R_\odot, t_1)$	1.9	2.4	4.45	5.4	1.7	1.2
$b(R_\odot, t_1)$	0.39	0.49	0.95	0.99	0.36	0.3
$I(R_\odot, t_1)$	1.5	2.1	6.2	4.9	2.0	1.9
$d[O/H]/dR(t_1)$	-0.031	-0.033	-0.024	-0.041	-0.027	-0.074
$d[Fe/H]/dR(t_1)$	-0.030	-0.048	-0.028	-0.044	-0.026	-0.067
SN II rate	0.007	0.009	0.015	0.017	0.008	0.004
SN Ia rate	0.002	0.004	0.008	0.008	0.003	0.002
$v_R(R_\odot, t_1)$	-0.66	-0.73	-0.94	-0.94	-0.98	-0.5

$m_{tot,1}$: final total mass in $m_\odot$; $m_{d,1}(R > 15)$: mass in the final disk located outside the truncation radius of the initial disk; $m_{b,1}$: final mass within the central 3 kpc identified with the bulge; l_*, l_g : scalelengths of the stellar disk and the gaseous disk in kpc; Ψ, I : star formation rate and gas infall rate I in $m_\odot$ pc^{-2} Gyr^{-1}; v_R: radial velocity of the viscous gas flow at $R_\odot$ in km s^{-1}. The abundance gradients are given for t_1 and $6 \le R \le 10$ kpc in dex kpc^{-1}; SN rates are given in SNe per yr.

* The ΣR-models are characterized by the viscosity parameters a, b and ν_0, while the Q-model is described by the velocity dispersion v_g of the gas (in km s^{-1}) and by the (dimensionless) star formation efficiency ϵ.

for the SFR. (But note that for other parameter sets, especially with $b - a = 1$, very similar model disks can be found; see paper 1). Model 1 is identical with model 1 in paper 1. Model 2 is similar to model 1, but it starts with an initial disk of smaller core radius, i.e. with a more centrally concentrated radial gas density distribution. In models 3 and 4 (corresponding to models 4 and 5 in paper 1), the gas infall fraction is as large as 0.95 and the infall timescale is long. For the sake of demonstration, model 4 allows also for infall-induced radial gas flows where a value of 0.8 was arbitrarily adopted for the ratio of the azimuthal velocity components of the infalling gas to the disk gas. Model 5 is also similar to model 1, but the ratio β of the star formation timescale to the viscous timescale is enhanced by a factor of 2. We have further considered a modification of model 1 (not contained in Table 1) with a strongly enhanced viscosity in the innermost disk over the last few 10^8 yr to simulate the effect of a central bar. (Such a property may bring the inner gas density profile of the model in better agreement with the observed profile of the Galactic disk within the innermost few kpc; see paper 1). However, at high redshift, this modification is not distinguishable from the original model and is therefore not discussed explicitely here. With regard to the infall parameters we have two groups of models: models 1,2,5, and 6 have an intermadiate fraction of infalling mass ($i = 0.5$) and a relatively short infall timescale ($t_i \approx t_1/2$), whereas models 4 and 5 have strong ($i = 0.95$) but slow ($t_i \approx 2\,t_1$) infall. Finally, model 6 is a Q-model predicting radial abundance gradients about twice as large as in the ΣR-models. The evolution of the radial profiles of the gas density, the SFR, and the relative iron abundance [Fe/H] for all six models is shown in Fig. 1.

3. The history of the star formation rate

The SFR as a function of look-back time can be used to derive the luminosity evolution which can be confronted with observational constraints. According to our current understanding, the global SFR density has significantly dropped from redshift $z \approx 1...2$ to the present (Madau et al. 1996, 1998; Gallego et al. 1998; Bechtold et al. 1998). At higher redshifts, an increase of the SFR density with decreasing z is indicated by the data, but the interpretation is uncertain due to the poorly constrained effects of extinction by dust. Cassé et al. (1998) have tested the SFR histories predicted by 8 very different galaxy evolution models against the observed UV, B and IR broad band comoving luminosity densities from the Canada-France-Redshift-Survey (Lilly et al. 1996) complemented by the Hubble Deep Field data (Connolly et al. 1997; Sawicki et al. 1997).

In Fig. 2, the total SFR and the total gas mass for the six model disks are shown as a function of redshift for an Einstein-de Sitter cosmological model with $H_0 = 50$ km s^{-1} Mpc^{-1} (see next section for the parameters of the cosmological model). The two different sets of infall histories clearly subdivide the sample of models into two groups: disks undergoing strong but slow infall show a steady *increase* of both the total SFR and

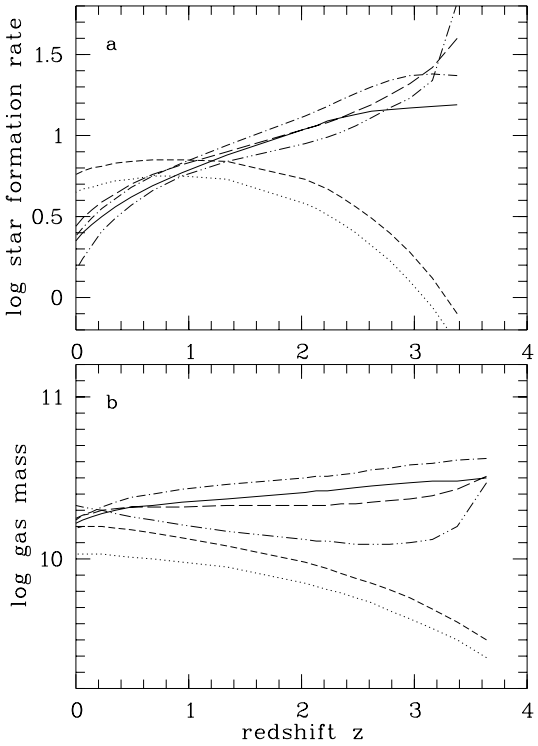

Fig. 2a and b. The total SFR in $m_\odot\ yr^{-1}$ **a** and the total gas mass in $m_\odot$ **b** as a function of redshift z for six disk evolution models from Table 1 (1-Solid, 2-long dashes, 3-short dashes, 4-dotted, 5-dash-dotted, 6-dash-dot-dot).

the gas mass with decreasing redshift while the corresponding curves are decreasing with decreasing z for the models with moderate infall. In the Q-model (moderate, slow infall), the total gas mass is strongly declining in the very beginning and is slowly increasing thereafter. The evolution of the SFR, predicted by the Q-model, is similar to that of the ΣR-models with moderate infall, with a stronger decline in the beginning, however.

We simply compare the SFR histories for our models from Fig. 2 with those of the models discussed by Cassé et al. shown in their Fig. 1. We find the high-redshift observations are very discrimatory with respect to the SFR history. Our moderate infall models (1,2,5,6) approximately correspond to their models 1a and 1b. For these models the luminosity density evolution is more similar to what corresponds to the multicolour data, though the observed decrease with decreasing z is even stronger. On the other hand, the star formation histories for our moderate infall models are comparable to that shown by Kennicutt (1998) for intermediate-type spirals (his Fig. 8). Kennicutt argues that the general difference between the redshift dependence of the volume averaged SFR and the typical SFR history of spiral galaxies probably reflects the importance of hierarchical processes such as mergers for the evolution of galaxies.

4. Frequency distribution of H I column densities $f(N, z)$

The two-dimensional distribution, $f(N, z)$, of dLyα systems in redshift z and neutral hydrogen column density N(HI) has been derived by Lanzetta et al. (1991, 1995) and Wolfe et al. (1995) from comprehensive statistical data. Wolfe et al. (1995) combined the results from a new dLyα survey with those from the Large Bright QSO survey (Hewett et al. 1995) to create a "statistical sample" of 62 dLyα systems with $N(\mathrm{H\,I}) \geq 10^{20}\,\mathrm{cm}^{-2}$. The improved statistics resulted in a new determination of $f(N, z)$ with considerably less scatter than was present in previous results, especially at high redshifts. The data clearly show a decline of the high column density systems with decreasing redshift. It has been emphasized by several authors (e.g. Wolfe et al. 1995; Khersonsky & Turnshek 1996; Kauffmann 1996; Prochaska and Wolfe 1997) that the present results can be used to place important constraints on the evolution of the absorber systems, despite our poor knowledge of the statistics at low z. In this section, the results from the Wolfe et al. study are confronted with the gas density evolution in the galaxy evolution models from Sect. 2. We describe the method and the assumptions to derive $f(N, z)$ from the models and present the comparison with the empirical data.

The probability that a line of sight intersects a galaxy with H I column density in the interval $(N, N+dN)$ at an absorption distance between l and $l + dl$ depends on the number density $n(L)$ of absorber galaxies, the cross section $d\sigma(N, l)$ of that part of the galaxy that corresponds to the column density interval $(N, N + dN)$, and the length dl of the absorption distance interval. The number of absorbers per sightline with H I column densities between N and $N + dN$ at redshift z is given by

$$f(N, z)dNdz = n(z(l))d\sigma(N, z(l))dl, \tag{4}$$

where dz is the redshift interval corresponding to dl. Integration of Eq. (4) yields the distribution $f(N)$ of absorber column densities within a given redshift interval:

$$f(N, z_1 \leq z \leq z_2) = \int_{z_1}^{z_2} \frac{d\sigma(N, z)}{dN} n(z) \frac{dl}{dz} dz. \tag{5}$$

The radial displacement function is given by

$$\frac{dl}{dz} = \frac{c}{H_0} \frac{1}{(1+z)E(z)}, \tag{6}$$

where $E(z)$ depends on the cosmological model (see e.g., Peebles 1993). Throughout the present paper we adopt the same cosmological parameters used by Wolfe et al. (1995) to obtain the empirical $f(N, z)$: a vanishing cosmological constant $\Lambda = 0$ and a deceleration parameter $q_0 = 0.5$, which yields $E(z) = (1 + z)^{3/2}$. Further, again following Wolfe et al., a present Hubble constant $H_0 = 50\,\mathrm{km\,s^{-1}\,Mpc^{-1}}$ and a constant comoving number density, n_0, of absorber galaxies are adopted, i.e. $n(z) = n_0(1 + z)^3$. The lookback-time $t_{lb}(z)$ is computed from integrating $dt_{lb} = dl/c$ with dl from Eq. (6).

The cross section $\sigma(N, z)$ is derived from the radial gas density profile, $\Sigma_g(R, t_{ev})$, predicted by the the galaxy evolution models at the evolution time $t_{ev}(z)$. Considering a face-on disk at redshift z, the cross section for the gas column density interval $(N_\perp, N_\perp + \Delta N_\perp)$ is given by

$$\sigma(N_\perp, \Delta N_\perp, z) = 2\pi R(N_\perp, z)|\Delta R(N_\perp, \Delta N_\perp, z)|, \tag{7}$$

where $R(N_\perp, z)$ and $\Delta R(N_\perp, \Delta N_\perp, z)$ are the galactocentric radius and the radial interval corresponding to the gas column density $N_\perp$ and the density interval $(N_\perp, N_\perp + \Delta N_\perp)$, respectively.

The distribution function, $f(N_\perp)$, for face-on disks is obtained from Eq. (5) in combination with Eqs. (6) and (7):

$$f(N_\perp, z_1 \le z \le z_2) = C \int_{z_1}^{z_2} R(N_\perp, z) \left| \frac{dR}{dN_\perp} \right| \sqrt{1+z}\, dz, \quad (8)$$

with $C = 2\pi c n_0 / H_0$. (For $z = 0$ and the special case of an exponential density profile, Eq. (8) is easily transformed into Eq. (20) in Wolfe et al. (1995).) Fall & Pei (1993) and Wolfe et al. (1995) have demonstrated how the distribution function accounting for inclination effects, $f(N)$, can be obtained from the distribution for face-on disks, $f(N_\perp)$. We adopted Eq. (21) in Wolfe et al. (1995) in combination with our Eq. (8) to derive $f(N, z)$ for the galaxy evolution models described above. The model gas column density, Σ_g, is transferred to the number column density N of H I atoms adopting a hydrogen fraction by mass of $X = 0.7$. In high-redshift dLyα absorbers, only small fractions of molecular gas have been observed (Black et al. 1987; Chaffee et al. 1988; Foltz et al. 1988; Levshakov et al. 1992; Srianand & Petitjean 1998). Ge & Bechtold (1997) found a H_2 gas mass fraction of ≈ 0.2 in a $z = 1.9731$ dLyα absorber. This is the by far largest molecular gas mass fraction known. Therefore, it seems reasonable to neglect the molecular gas phase in the high-redshift systems. The fraction of ionised hydrogen is neglected as well. Then we have $N_{\rm HI} = 0.9\,10^{20}\,\Sigma_g$, if $N_{\rm HI}$ is given in units of atoms per cm^2 and Σ_g in $m_\odot$ pc^{-2}.

We start with the "diffeomorphic" approach (Timmes et al. 1995a), i.e. we assume that all dLyα systems have nearly the same history as the disk of our Galaxy. The results for the H I column density evolution are shown in Fig. 3. The style of representation is the same as in Wolfe et al. (1995). There is a clear difference between strong and moderate infall ΣR-models: For strong & slow infall, the gas column density and the SFR in the initial disk are lower, and radial gas flows are less efficient to concentrate gas toward the centre. In the high column density range, the distribution function $f(N, 2.5 \le z \le 3.5)$ is therefore considerably steeper in these models than in moderate infall models. On the other hand, moderate infall models predict too a shallow distribution $f(N, 2.5 \le z \le 3.5)$ which also fails to fit the empirical data perfectly. Nevertheless, moderate infall models clearly show the steepening of $f(N)$ with decreasing z which seems indicated by the empirical data. The Q-model is apparently inconsistent with the observations as it predicts too few dLyα absorbers of low column density as a direct consequence of the flat gas density profiles in the outer disk in this model (Fig. 1). A reasonable fit to the observed gas column density evolution in dLyα absorbers is expected for ΣR-models with infall properties between the two infall types. However, it seems more appropriate to consider the effects of a non-diffeomorphic approach prior to such a fine tuning.

In order to involve a mass spectrum of dLyα absorber galaxies, the gas density evolution has to be known for galaxies of different baryonic mass, m. Unfortunately, good-fit models are available only for the Milky Way disk ($m = m_{MW}$). Therefore, we have to adopt a very simplified approach: We assume *(1.)* that the mass ratio $\mu = m/m_{MW}$ does not change with z for any dLyα galaxy with mass m and *(2.)* that the gas column density approximately scales with μ for galaxies with different m at fixed z, i.e. $\Sigma_g(R, \mu) = \mu \Sigma_g(R, \mu = 1)$. Then, the distribution $f(N)$ of dLyα column densities is obtained from

$$f(N) = \int_0^\infty \Phi(\mu) \frac{f(N, \mu)}{n_0} d\mu, \quad (9)$$

where $f(N, \mu)$ is computed as explained above. The distribution of the mass ratio, $\Phi(\mu)$, is obtained from $\Phi(\mu)\, d\mu = \Phi(L/L_*)\, d(L/L_*)$, where $\Phi(L/L_*)$ is the luminosity function (LF) expressed in terms of a characteristic luminosity L_*. Adopting a similar and constant baryonic mass-to-luminosity ratio for all dLyα galaxies we have $\Phi(\mu) = \Phi(L/L_*)/\mu_*$ with $\mu_* = L_*/L_{MW}$. Note that only the shape of the LF is adopted to be conserved, whereas the luminosities of the galaxies itself are allowed to evolve with z (cf. e.g., Brinchmann et al.1998).

For most samples of field galaxies the total LF is well represented by a Schechter (1976) form with a faint-end slope $\alpha \approx -1.0$ to -1.5 (e.g. Ellis et al. 1996; Zucca et al. 1997; Marzke et al. 1998). However, as has been observed in many galaxy samples, the LF does appear to depend on various galaxy properties, especially on morphology (Sandage et al. 1985; Binggeli et al. 1988; Marzke et al. 1994; Lilly et al. 1995; Heyl et al. 1997; Lin et al. 1997; Marzke et al. 1998; Brunzendorf & Meusinger 1999). The faint end of the LF of any type of galaxies is difficult to measure and is, therefore, affected by considerable uncertainties. Tammann (1986) found that the luminosity function of nearby spirals, expressed in terms of absolute magnitudes M, is well represented by a Gaussian with $\Phi_* = 2\,10^{-3}$ Mpc^{-3}, $M_* = -17.8$, $\sigma_M = 1.8$. According to the results from the CfA redshift survey (Marzke et al. 1994) the type-specific LF for Sa-Sd types is a Schechter function decreasing at the faint end with $\alpha = -0.81$, $M_* = -18.76$, $\Phi_* =$

Table 2. Space number densities (Mpc^{-3}) of dLyα galaxies at the present time, derived from the fit of the column density distributions in Figs. 3 and 4, respectively. (n_0: number density of Milky Way type galaxies from the diffeomorphic approach in Fig. 3; Φ_*: parameter of the Gaussian LF used in Fig. 4.)

model	1	2	3	4	5	6
n_0	0.015	0.020	0.022	0.040	0.017	0.015
Φ_*	0.005	0.007	0.012	0.015	0.004	0.008

Table 3. Parameters of the Schechter type mass function used in Fig. 5.

model	a	b	c	d	e	f
α	0.8	1.2	1.4	1.2	1.2	1.2
μ_*	1.0	1.0	1.0	2.0	1.0	0.5
μ_{min}	0.01	0.01	0.01	0.01	0.1	0.01
Φ_*	0.008	0.004	0.003	0.004	0.007	0.006

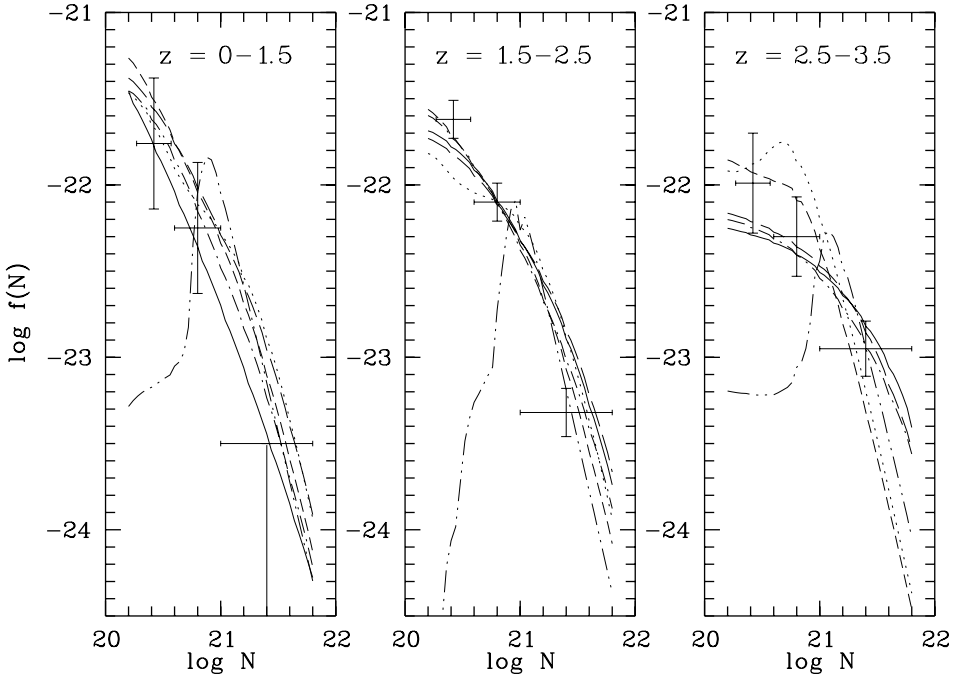

Fig. 3. The frequency distribution of H I column densities of QSO absorbers in three redshift intervals. The empirical data (Wolfe et al. 1995) are represented by crosses where the horizontal bars indicate the bin sizes and the vertical bars are the errors estimated from Poisson statistics. The model results are given by curves (as in Fig. 2) which are, in general, normalized to fit the intermediate observational data point in the z interval $1.5 \leq z \leq 2.5$.

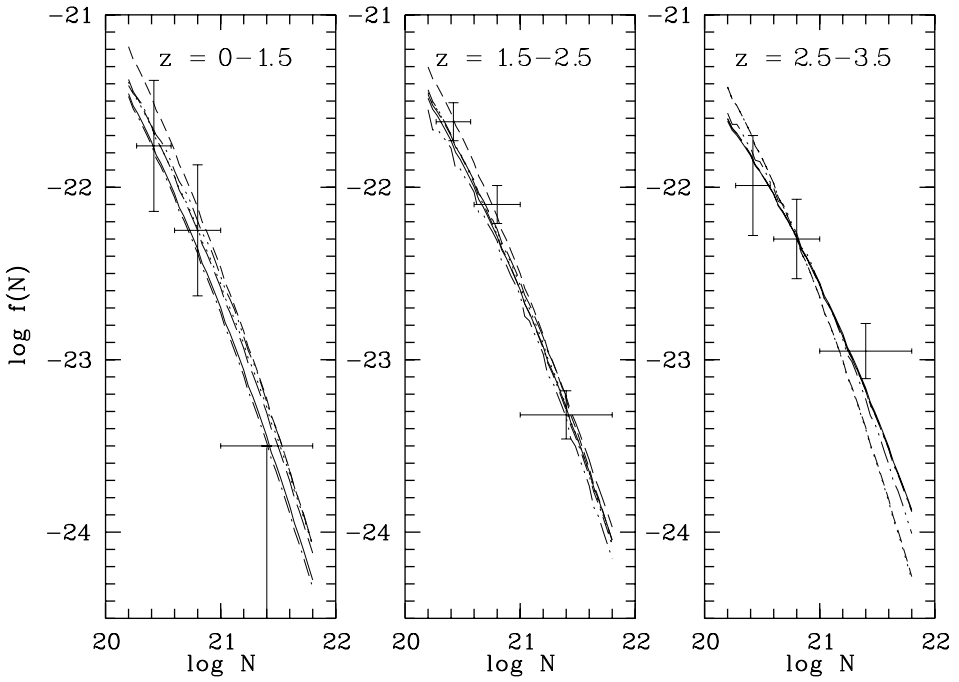

Fig. 4. As in Fig. 3 but the model distributions are weighted with the Gaussian LF for spiral galaxies from Tammann (1986). The curves are normalized to fit the intermediate data point in the highest redshift bin.

$0.0015\,\mathrm{Mpc}^{-3}$. The faint-end slope of the spiral LF derived from the Second Southern Sky Redshift Survey is essentially flat (Marzke et al. 1998). Also the rest-frame B-band LF of high-redshift galaxies selected by having produced absorption in the spectra of background QSOs resembles a Gaussian rather than a standard Schechter function (Steidel 1995).

We use Tammann's LF for spirals to compute $f(N)$ according to Eq. (9) for the six models from Table 1. Alternatively, a Schechter function was adopted with different parameter sets listed in Table 3. The results are shown in Figs. 4 and 5, respectively. For technical reasons, the μ-integration is performed on a logarithmic scale and the integration interval was restricted to the range $\log \mu = -2$ to +1. The results do not change significantly when the upper limit is increased. For a Schechter function with a steep faint-end slope ($\alpha < -1$), however, $f(N)$ at high redshift becomes very steep for a lower limit $\log \mu < -1$. On the other hand, decreasing the lower mass limit does not significantly affect the results for the Gaussian from Tammann (1986) as well as for the Schechter function from Marzke et al. (1994) for spirals.

It is noteworthy that the consideration of the mass function has a significant effect on the resulting column density distri-

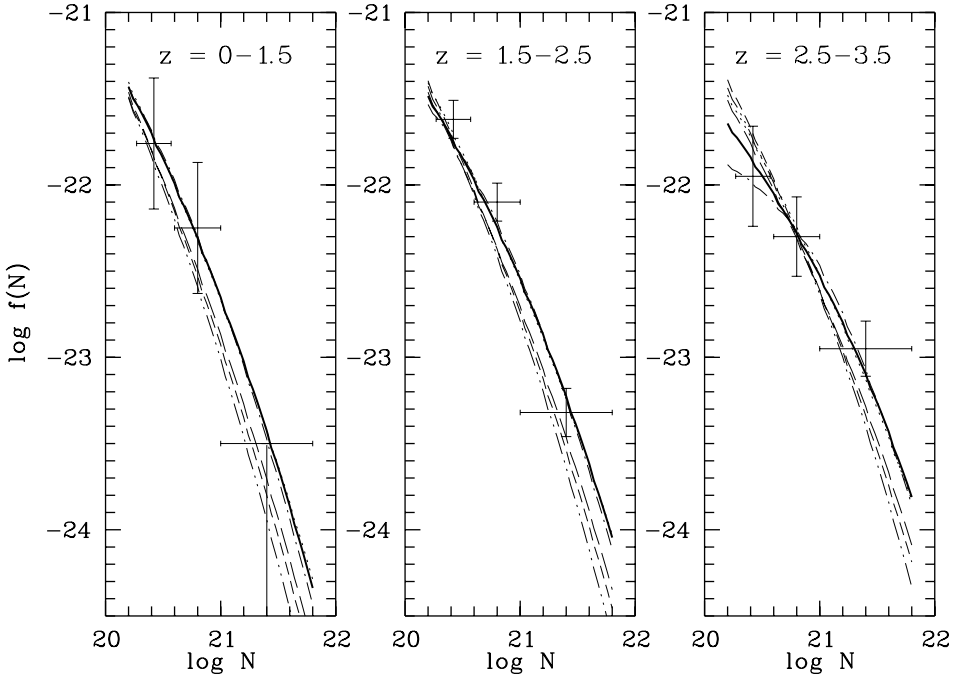

Fig. 5. As in Fig. 3, but the model distribution is shown only for model 1, weighted with a Schechter LF with different parameter sets listed in Table 3. (a–solid, b–long dashes, c–short dashes, d–dotted, e–dash-dotted, f–dash-dot-dot).

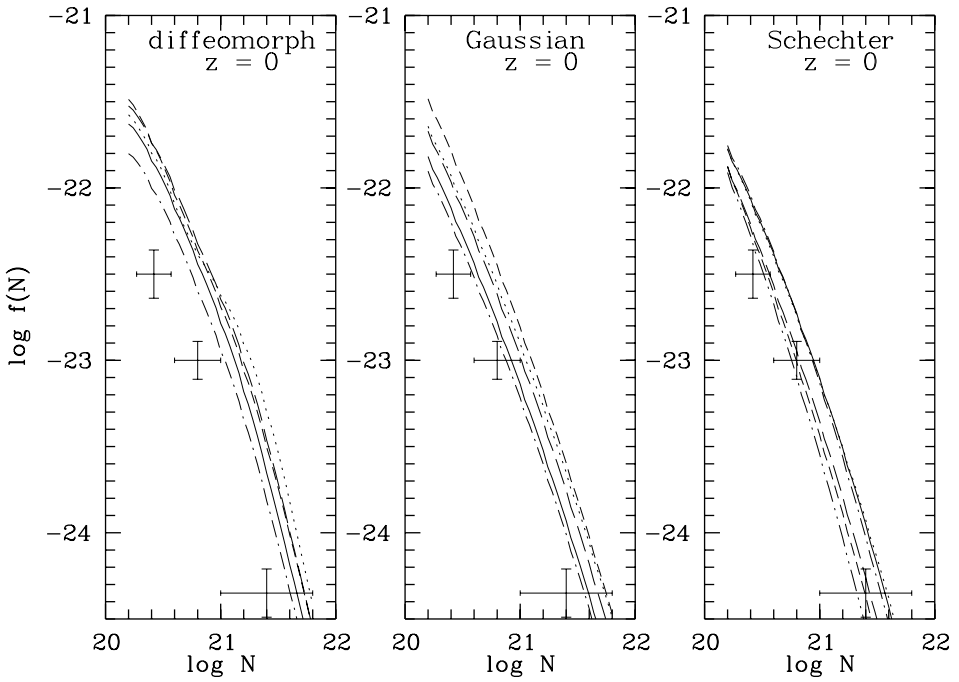

Fig. 6. The frequency distribution of H I column densities as predicted from the models for $z = 0$. The empirical data are based on 21 cm surveys of nearby galaxies (taken from Khersonsky & Turnshek 1996). From the left to the right, the curves have the same meanings as in Figs. 3, 4, and 5, respectively.

bution $f(N, z)$, especially at highest redshifts. This effect is of about the same order of magnitude as the use of different galaxy evolution models (compare Fig. 4 with Fig. 5). The observational data appear to be well fit for the spiral LF, provided that the faint end is decreasing. If it is not, a good fit can be achieved only if low-mass ($m < 0.1 m_{MW}$) disks are assumed to be much more compact than the more massive ones. Note especially, that even the Q-model provides a reasonable fit to the observations after weighting with the LF (Fig. 4).

The H I content at $z = 0$ is obtained from 21 cm observations of nearby gas-rich galaxies in the local Universe, especially from spirals which appear to contain the overwhelming majority of H I at present, on the conditions that *(1.)* very little gas is outside the normal galaxies and *(2.)* the population and space density of the nearby galaxies is typical for the present Universe. Based on the data sets from Rao & Briggs (1993) and Fall & Pei (1993), Khersonsky & Turnshek (1996) studied the evolution of the H I column density distribution down to $z = 0$. We adopt the data points and error bars given in their Fig. 1 to confront our model predictions with the empirical $f(N)$ at $z = 0$. As pointed out by Rao & Briggs, a complete tally of mass at $z = 0$ would also find substantial molecular gas comparable to the mass in H I.

From the data on 53 Sa to Sc type spirals listed by Kennicutt et al. (1994) we find a mean $\log m_{HI}/m_{H_2}$ of 0.11 ± 0.61, and we assume therefore that about half of the mass of interstellar hydrogen is in the form of H_2 in present-day spirals (cf. Casoli et al. 1998). Fig. 6 shows the distributions of H I absorber densities at $z = 0$ after correction for the molecular gas fraction. The observational data are fit only for a Schechter LF, but only for such parameters where the predicted number of high-redshift dLyα galaxies with $\log N = 21...22$ is a factor of more than two lower than observed. The other way round, if the models are required to match the observed column density distribution at high redshift, the predicted number density of absorbers at $z = 0$ is approximately a factor of two higher than what is expected from H I surveys of nearby galaxies.

5. Metallicity evolution

Chemical abundances in dLyα absorber systems have become available by a variety of studies (Black et al. 1987; Meyer & York 1987; Chaffee et al. 1988; Meyer et al. 1989; Meyer & Roth 1990; Rauch et al. 1990; Pettini et al. 1990; Meyer & York 1992; Fan & Tytler 1994; Pettini et al. 1994; Wolfe et al. 1994; Green et al. 1995; Pettini et al. 1995a; Steidel et al. 1995; Lu et al. 1996; Molaro et al. 1996; Pettini et al. 1997; Prochaska & Wolfe 1997; Molaro et al. 1998; Boissé et al. 1998; Pettini et al. 1999a,b). The rôle of dust for the derived elemental abundances has been investigated by Vladilo (1998). Matteucci et al. (1997) presented a detailed comparison of dLyα abundances and abundance ratios with the predictions from chemical evolution models of galaxies of different types. In order to explain the high N/O ratio observed in two dLyα systems Matteucci et al. conclude that these systems resemble dwarf galaxies rather than spirals.

Pettini et al. (1990) first drew attention to the diagnostic value of Zn as a metallicity tracer in dLyα systems: *(1.)* The abundance ratio [Zn/H][1] measures chemical enrichment analogously to the "classic" metallicity tracer [Fe/H]; for stars in the Galaxy [Zn/Fe] is nearly solar, independent of [Fe/H]. *(2.)* Accurate abundance determination of Zn is possible from non-saturated lines for most dLyα absorber sytems. *(3.)* The abundance ratio [Cr/Zn] directly measures the depletion onto dust grains. *(4.)* Corrections for a missing fraction of Zn are small because it is mostly singly ionised in H I regions and shows little affinity for dust. Pettini et al. (1997) presented Zn abundances for a sample of 34 dLyα systems. The redshift-metallicity relation derived from these data is characterized by a "plateau" near one tenth solar metallicity between $z \approx 1...3$ and by a large metallicity scatter at fixed redshift. For $z > 3$, the mean metal abundance is observed to be lower than in all other z intervals (cf. also the [Fe/H] data of Lu et al. 1996), and it is tempting to interpret the increase in metal abundances at $z \approx 3$ as indication of the onset of star formation in galaxies (Pettini et al. 1997). At low redshift, there is no trend in these data to approach solar metallicity. Pettini et al. (1997) have pointed to the possibility that the missing evidence for chemical enrichment at low redshifts may be an effect of small number statistics, given especially the heavy weight of a low-metallicity, low-surface brightness absorber galaxy in this subsample. Indeed, Boissé et al. (1998) found that the revised mean [Zn/H] at low z is more consistent with the picture of an continuously increasing metallicity as z goes to zero after they have included three new Zn abundance estimates. Pettini et al. (1999a) have compiled Zn abundances for further four dLyα systems with $z < 1.5$. In combination with other published data they found again no significant evolution of [Zn/H] towards low z.

In the present paper, we have to confront the observed column density-weighted mean zinc abundances $[\langle \mathrm{Zn/H} \rangle]$ and the abundance scatter $\sigma_{[\mathrm{Zn/H}]}$ with the predictions from our chemical evolution models (paper 1). For $z > 1.5$ we adopt the observational data from Pettini et al. (1997). At low redshifts ($z \leq 1.5$), we computed $[\langle \mathrm{Zn/H} \rangle] = -0.88$ and $\sigma_{[\mathrm{Zn/H}]} = 0.43$ from the combination of the data for four systems given by Pettini et al. (1997), four systems given by Pettini et al. (1999a), three systems (Q 0809+483, Q 1209+107, Q 1229-021) given by Boissé et al. (1998), and for two systems quoted also by Pettini et al. (1999a), namely Q 1622+238 (Steidel et al. 1997) and Q 1122-168 (de la Varga & Reimers 1998). This value for $[\langle \mathrm{Zn/H} \rangle]$ is between the higher value from Boissé et al. and the somewhat lower value given by Pettini et al. (1999a) and idicates only a very slow metallicity evolution with decreasing z.

We consider the diffeomorphic approach only since chemical evolution models are available only for our Galaxy. First, we use the [Fe/H] data from the models, which were shown (paper 1) to match both the observed age-[Fe/H] relation and the [Fe/H] distribution of the long-lived stars in the solar neighbourhood, and apply the empirical relationship between observed zinc and iron abundances from Galactic disk and halo stars. Sneden et al. (1991) studied the zinc abundances of 23 field dwarfs and 18 field giants using high-resolution, low-noise spectra. They found a nearly solar zinc-to-iron ratio [Zn/Fe] $= 0.04 \pm 0.01$ dex over the entire metallicity range [Fe/H] $= -2.9... - 0.1$. The result is quite robust and is in excellent agreement with the earlier result by Luck & Bond (1985), but the scatter could be significantly reduced by the work of Sneden et al. (1991). Thus, the computed iron abundances are translated to zinc abundances by

$$[\mathrm{Zn/H}] = [\mathrm{Fe/H}]_{model} + \overline{[\mathrm{Zn/Fe}]} + \delta_{\mathrm{Zn},dL\alpha}, \qquad (10)$$

with $\overline{[\mathrm{Zn/Fe}]} = 0.4$. Dust depletion is taken into account by the term $\delta_{\mathrm{Zn},dL\alpha}$ with $\delta_{\mathrm{Zn},dL\alpha} = -0.08... - 0.19$ according to the study of dust and elemental abundances in dLyα systems by Vladilo (1998). We apply Monte Carlo simulations to allow for random positions and inclinations of the model disks relative to the sightline and for selection effects (see below). The method is described in the Appendix.

In Fig. 7, the resulting redshift-metallicity([Zn/H]) relations for the 6 models from Table 1 are shown for $\delta_{\mathrm{Zn},dL\alpha} = -0.08$ (left) and -0.19 (right), respectively. The scatter $\sigma_{[\mathrm{Zn/H}]}$ at fixed redshift is shown separately in the bottom panels to avoid overcrowding. As can be seen from the upper part, the relations

[1] The conventional notation is used where $[\mathrm{X/Y}] = \log(\mathrm{X/Y}) - \log(\mathrm{X/Y})_\odot$.

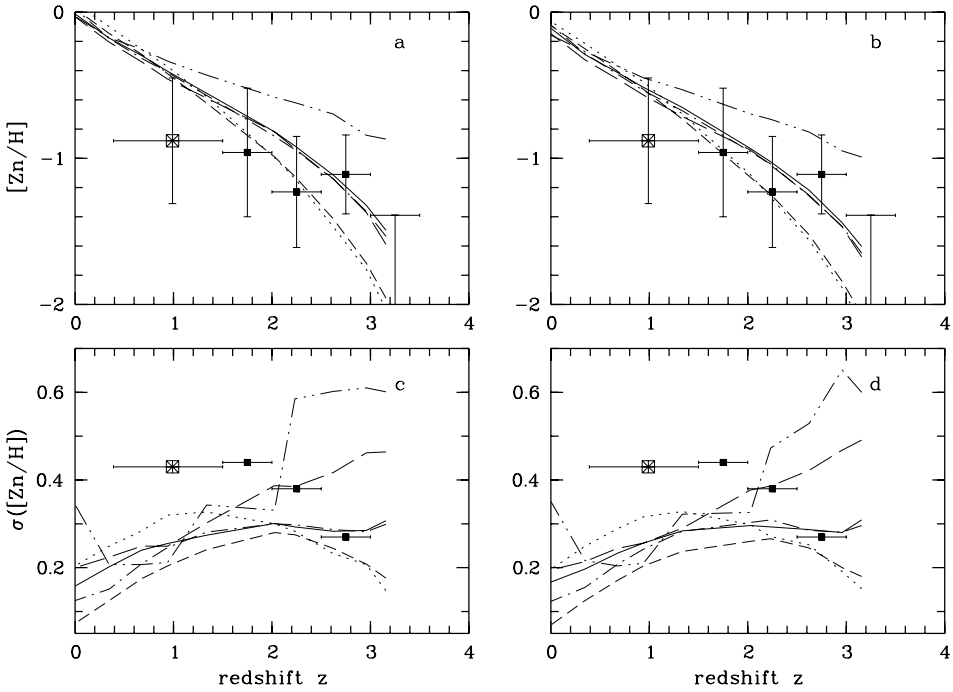

Fig. 7a–d. Redshift-metallicity ([Zn /H]) relations (**a** and **b**) and redshift-metallicity scatter relation (**c** and **d**) for the models from Table 1 from Monte Carlo simulations (curves; the line styles have the same meaning as in Fig. 2). The zinc abundances in the model disks were calculated from predicted iron abundances adopting the mean [Zn/Fe] abundance ratio from Galactic low-metallicity stars and were corrected for depletion onto dust grains according to Vladilo (1998) with dust depletion $\delta_{Zn,dL\alpha} = -0.08$ (**a** and **c**) and -0.19 (**b** and **d**), respectively. The observational data are taken from Pettini et al. (1997) for $z > 1.5$. The lowest z data point includes the zinc abundance determinations from Pettini et al. (1997, 1999a), Steidel et al. (1997), Boissé et al. (1998), and de la Varge & Reimers (1998). In the highest z bin, only upper limit abundance data are available.

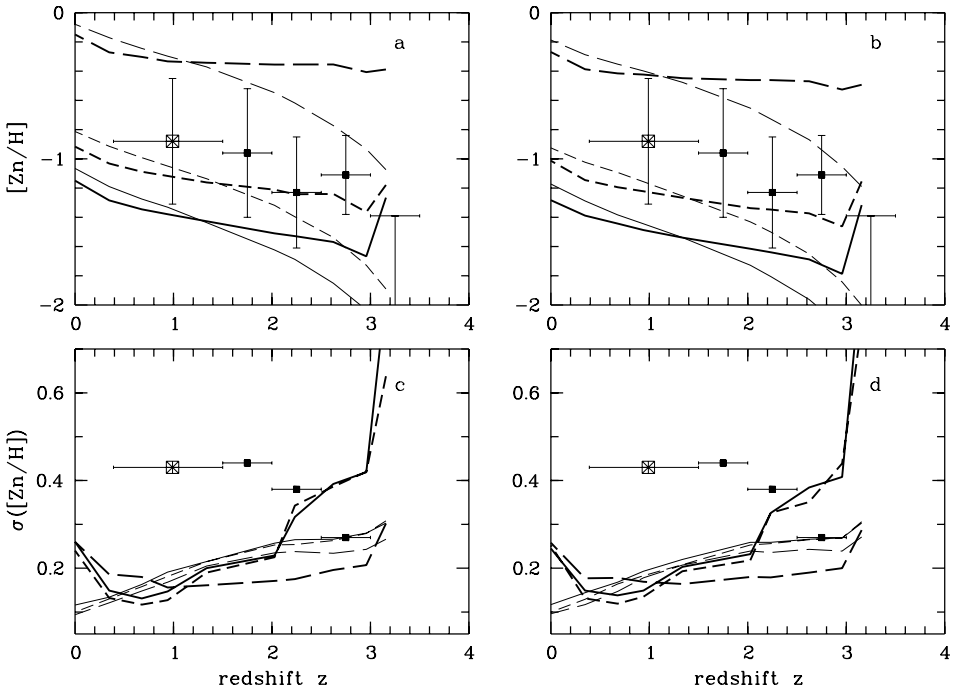

Fig. 8a–d. As Fig. 7, but with zinc abundances computed from different sets of theoretical Zn production rates in massive stars: solid – Nomoto et al. (1997a), long dashes – Woosley & Weaver (1995) for $Z_\odot$, short dashes – Woosley & Weaver (1995) for metallicity-dependent production rates. The thick curves are for model 6, the thin curves for model 1.

predicted from moderate infall ΣR-models are in near agreement with observations for $z > 1.5$ while the two strong infall ΣR-models predict too a steep increase of metallicity with decreasing z for $z > 2$. The trend of steeply increasing metal abundance at $z > 3$ is best expressed by the moderate infall models with standard initial disk (models 1,5,6). At low redshifts, the ΣR-models predict a stronger increase in metallicity than is observed. The smaller slope of the z-[Zn/H] relation for the Q-model is in better agreement with the observed slope. However, the abundances predicted by this model are too high.

In principle, the use of theoretical stellar yields for zinc production provides the more direct way to model the redshift evolution of Zn, especially if the star formation history for a typical dLyα absorber is different from that of the Milky Way. (For instance, Molaro et al. (1998) found evidence that the chemical evolution of the dLyα at $z = 2.309$ towards PHL 957 is different from the evolution of the Galaxy.) Stellar Zn yields for massive stars are given by Nomoto et al. (1997a) for stars of solar initial metallicity and by Woosley & Weaver (1995) for a set of different metallicities, respectively. The most important source

of uncertainties of the Zn yields is the mass cut for core collapse supernovae (Nomoto; private communication). Timmes et al. (1995b) notice that the high production of ^{68}Zn in the Woosley & Weaver models may be due to the parametrization of the SN explosion, or simply a consequence of the fact that the nuclear reaction network was terminated at germanium. We have computed the evolution of [Zn/H] using the stellar yields from Nomoto et al. and from Woosley & Weaver, respectively, for the same chemical evolution model. Zinc yields for SN Ia were taken from Nomoto et al. (1997b). The results are shown in Fig. 8 for the models 1 and 6. We find a difference of about 1 dex between the resulting [Zn/H] values from the two sets of input data, independent of z and of the disk evolution model. The Nomoto et al. (1997a) data generally predict too low Zn abundances, while too much Zn is produced with the Woosley & Weaver yields. (We have used their model A; for models B and C the predicted Zn yields are even higher.) As noticed by Timmes et al. (1995b), there is no contribution to zinc abundance evolution due to intermediate- and low-mass stars, and standard models for type Ia supernovae produce little zinc. Thus, the difference in the results immediately reflects different stellar yields for Zn production in massive stars. We suspect that zinc abundances in models of Galactic chemical evlolution are much more uncertain when computed from the available theoretical Zn yields than when derived from Fe abundances using the empirical [Zn/Fe] ratio for Galactic stars. (We emphasize that the primary goal of this section is to confront dLyα systems with models for the Galactic disk.)

The large scatter of the abundance of heavy elements in dLyα absorbers at comparable redshifts is a striking property of the redshift-metallicity relation. Lu et al. (1996) have discussed iron abundances and considered it likely that the large spread in [Fe/H] is due to different formation epochs of the sample galaxies and/or due to a heterogeneous mix of galaxy types. However, the analysis of [Fe/H] is complicated by the fact that this ratio depends stronger on the dust content than [Zn/H] (Pettini et al. 1997). In the lower part of Fig. 7, we compare the observed standard deviation $\sigma_{\rm [Zn/H]}$ with that one computed from the disk evolution models. There is no significant difference for $z > 2$. At lower and intermediate redshifts, the scatter in the ΣR-models is too small by a factor of about 1.5 to 2. The Q-model predicts a larger scatter at high redshift and at present. The increased standard deviation at $z \approx 0$ is clearly due to the stronger radial abundance gradient in this model. However, as the gradient increases with time (Fig. 1), the scatter predicted for the redshift range $z \approx 0.5...2$ seems too low also for the Q-model. It is tempting to interpret the difference beween the predicted and the observed scatter as due to different types of spiral galaxies having different star formation timescales (Kennicutt et al. 1994) and, therewith, different chemical histories.

The ratio of alpha to iron-peak element abundances has been discussed in the context of the chemical evolution of dLyα systems in several studies (e.g., Timmes et al. 1995a; Lu et al. 1996; Matteucci et al. 1997; Vladilo 1998; Pettini et al. 1999b). Due to the different lifetimes of the progenitor stars of SN II and SN Ia the [α/Fe] abundance ratio is an important indicator of the chemical evolutionary stage: While the solar ratio, which is typical of a progressed stage in Galactic disk evolution, is explained by the cumulative effect of both SN types, the early evolution should be dominated by the nucleosynthesis products from SN II characterized by a relative enhancement of alpha elements (Tinsley 1980; Matteucci & Francois 1989; Wyse & Gilmore 1993; Matteucci et al. 1997). Because oxygen abundances are generally uncertain in dLyα absorbers (see Matteucci et al. 1997), silicon has been taken as a tracer of alpha elements (Pettini et al. 1995a; Vladilo 1998).

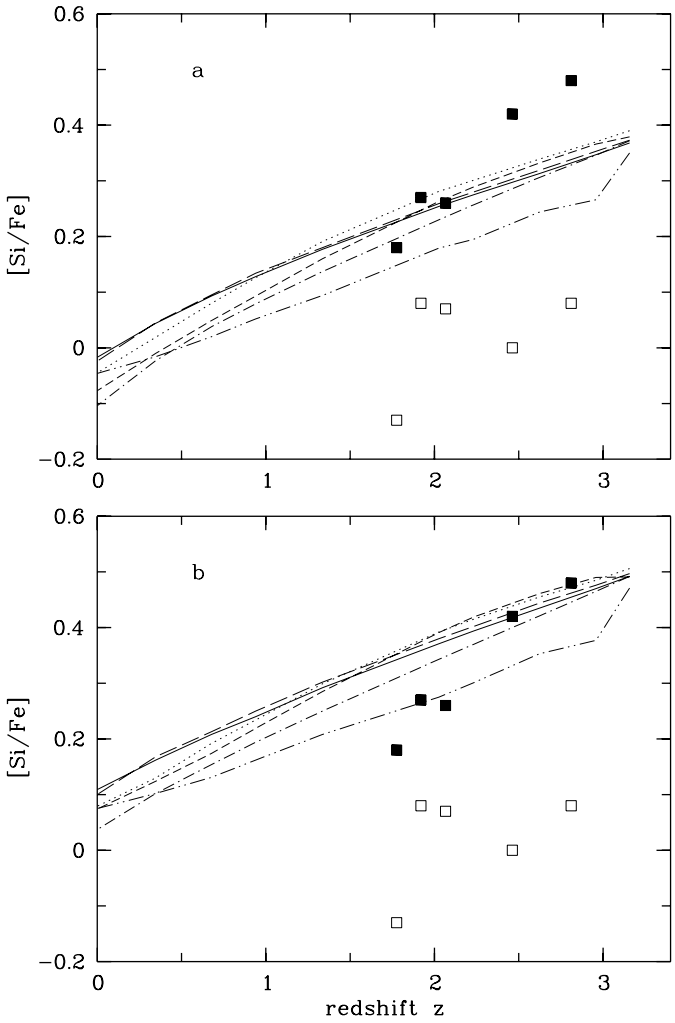

Fig. 9a and b. The element abundance ratio [Si/Fe] as a function of redshift for the six models from Monte Carlo simulations (curves as in the previous figures). The model Si abundances were calculated in **a** from the predicted oxygen abundances adopting the mean [Si/Fe]-[O/Fe] relation from Galactic disk and halo stars and in **b** from Si production rates for massive stars from Nomoto et al. (1997a) and for SN Ia from Nomoto et al. (1997b). The uncertainties are typically $\sigma_{\rm [Si/Fe]} \approx 0.1$ dex at low redshift and 0.05 dex at high redshift for the ΣR-models and 0.10 and 0.15 dex for model 6, respectively. The observed abundance ratios for five dLyα systems (filled squares) as well as the dust-corrected ratios (open squares) were taken from Vladilo (1998).

In a first attempt, we adopt an empirical transformation relation for Galactic disk and halo stars is adopted to transform the computed [O/Fe] model abundances to [Si/Fe]: From the abundance data for 29 stars with [O/Fe] = 0...0.4 (disk and halo) given by Nissen & Schuster (1997) we found by linear regression [Si/Fe]$= 0.76(\pm 0.08)$ [O/Fe]. As an independent approach, we use the stellar yields from Nomoto et al. (1997a) for explosive Si production in massive stars and from Nomoto et al. (1997b) for the contribution by supernovae of type Ia (i.e. the same models as have been used for the calculation of iron abundance evolution in paper 1) to compute the abundance ratio [Si/Fe]. The resulting redshift-[Si/Fe] relations are shown in Fig. 9, compared with the observed silicon abundances in five dLyα systems, along with the corresponding dust-corrected values (Vladilo 1998). According to Vladilo, the total random error in the observed abundances is expected to be smaller than 0.15 dex.

Unfortunately, the interpretation of Fig. 9 strongly depends on the question of dust depletion. The observed silicon overabundance in dLyα absorbers is in agreement with the model predictions, i.e. with enrichment dominated by type II SN, if there is only a small amount of dust depletion, as was emphasized by Lu et al. (1996). However, the agreement disappears completely after corrections for dust depletion according to Vladilo are applied. The disk model predictions are clearly inconsistent with a nearly solar [α/Fe] ratio at high redshift. Further evidence for solar-like abundance ratios in dLyα systems is discussed by Vladilo (1998) and Pettini et al. (1999b).

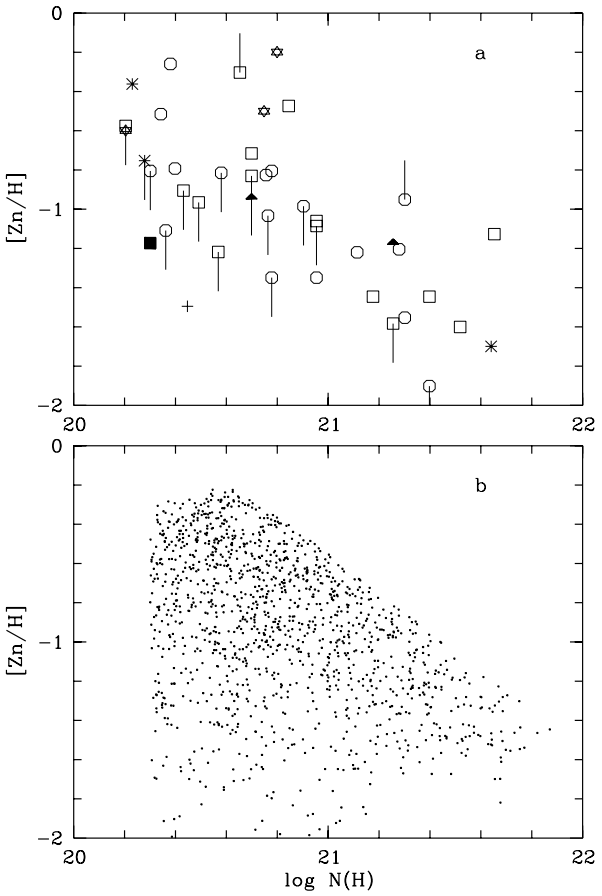

Fig. 10a and b. Zinc abundances ([Zn/H]) of dLyα absorbers in dependence on the hydrogen column density **a** for the systems used here to study the chemical evolution of dLyα systems (filled triangles: Meyer et al. 1989; open squares: Pettini et al. 1994; open circles: Pettini et al. 1997; filled square: Steidel et al. 1997; stars: Boissé et al. 1998; plus sign: de la Varge & Reimers 1998; asterisks: Pettini et al. 1999a), and **b** for systems with $N(\mathrm{Zn}) \leq 1.4\,10^{13}\,\mathrm{cm}^{-2}$ from Monte Carlo simulations of 10 000 sightlines for model 1.

6. Dust extinction bias

Though it may be true that the mean dust-to-gas ratio in high-redshift dLyα systems is on average lower than in nearby spirals (Fall et al. 1989; Pei et al. 1991; Pettini et al. 1994; Vladilo 1998), it seems likely that the statistics of dLyα absorbers is biased against systems with the highest dust-to-gas ratio. The existence of such a bias was first indicated by the finding of Pei et al. (1991) that QSOs behind dLyα systems have on average steeper spectra than QSOs without dLyα absorption. More recently, Boissé et al. (1998) have pointed out that there is a clear deficiency of systems with both large hydrogen column density and high metallicity, contrary to what is expected if there is no bias due to dust extinction. When all available measurements are considered in the [Zn/H]-log $N(\mathrm{H})$ diagram, there appears a maximum zinc column density $N_{max}(\mathrm{Zn}) = 1.4\,10^{13}\,\mathrm{cm}^{-2}$ (Boissé et al. 1998; see also Fig. 10). Since zinc is a good tracer for the total amount of metals it is also a good indicator of the possible amount of dust. Thus, the deficiency of systems beyond the dividing line is very likely due to the bias introduced by extinction of the QSO light by dust-rich absorber systems; a definitive view can be provided only on the basis of the investigation of dLyα systems from the spectra of fainter QSOs (Boissé 1995; Boissé et al. 1998).

There is no indication for a deficiency of systems with large N(Zn) in our simulations without further restrictions. In order to simulate the effect of the observational bias against systems with large N(Zn) we introduce the constraint $N(\mathrm{Zn}) \leq 1.4\,10^{13}\,\mathrm{cm}^{-2}$ (Fig. 10) before we compare the model results with observations. The resulting redshift-[Zn/H] relation is shown in Fig. 11. The agreement of the model predictions with observations is improved, mainly because the bias is especially strong at $z \approx 1$ (cf. Boissé et al. 1998). The [Si/Fe] abundance ratio is only weakly changed due to such a bias, and only at low redshifts.

On the other hand, the scatter in [Zn/H] is considerably reduced, especially at lower redshift, after the systems with high Zn column densities are removed. However, as the predicted mean [Zn/H] is increasing with decreasing z, the expected scatter in binning intervals may be larger than predicted by the curves in the lower part of Fig. 11. In Fig. 12, the total expected standard deviation $\sigma_{\mathrm{[Zn/H]}}$ is shown for the z intervals of the empirical data in Figs. 11. In the simulations shown in Fig. 12, we have also included an additional scatter $\sigma_{\mathrm{[Zn/H]},ice} = 0.15$ dex in the interstellar medium of the absorber galaxy, at fixed age and fixed galactocentric distance, due to inhomogeneous chemical evolution (see paper 1). However, the resulting scatter of

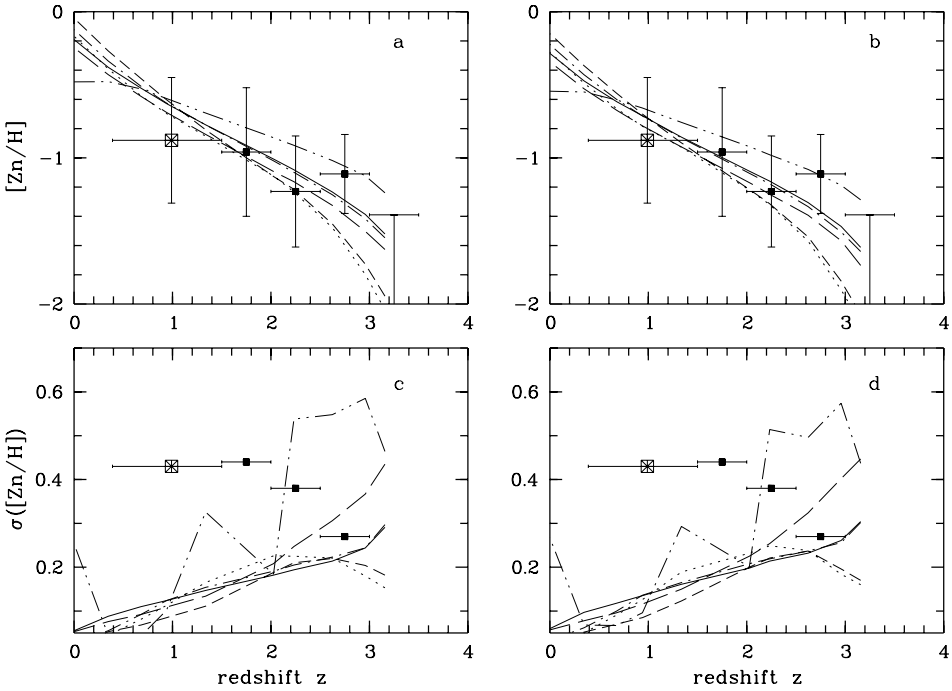

Fig. 11a–d. As Fig. 7, but the dLyα systems with zinc column densities $N(\mathrm{Zn}) > 1.4\,10^{13}\,\mathrm{cm}^{-2}$ are excluded.

the model abundances is still too small at intermediate and low redshifts even after these two effects are taken into account, especially for the Q-model with its small slope of the [Zn/H]-z relation. We guess that the difference between the observed and the predicted scatter is most likely due to a morphological mix of the absorber galaxies.

Fig. 13 demonstrates the effect of the dust selection bias on the redshift evolution of the distribution $f(N)$ of absorber column densities. It is clearly seen that $f(N)$ becomes steeper with decreasing redshift due to the bias, as was first noted by Fall & Pei (1993). As a consequence, only a small fraction of the high H I column density systems at $z < 1.5$ can be explained by spirals represented by our models. The remaining systems must be relatively metal-poor because of the constraint for N(Zn). Their consideration would, therefore, decrease the predicted mean metallicity at low redshift and increase the metallicity scatter, perhaps bridging the gap between the predictions and the observational data.

7. Discussion

There are strong indications that the available data on dLyα sytems are affected by the presence of dust (Pei et al. 1991; Boissé et al. 1998). Dust extinction produces a selection bias against high column density and high metallicity systems (Sect. 6). We find an improved fit of the observed redshift-[Zn/H] relation in simulations when such a bias is taken into account. This agreement may be taken as an indication that the metallicity evolution of many dLyα absorbers is similar to that predicted by the models for the Galactic disk, at least for the iron group elements. On the other hand, the observed abundance scatter at fixed redshift is then larger than that predicted by the Galactic disk models if the dust extinction bias is accounted for (Sect. 6). This can be naturally understood if dLyα systems are associated with various galaxy types with slightly different chemical histories. Such an interpretation is supported by the fact that the agreement of the model predictions with the observed H I column density evolution is improved after the diffeomorphic approach was replaced by the attempt to involve a mass spectrum of absorber galaxies (Sect. 4). Above all, the sample of the observed dLyα systems is expected to contain galaxies which are, at intermediate and low redshifts, chemically less evolved than the Galactic disk.

There arises a general problem for the predicted number densities of absorber galaxies when the high-redshift data are compared with data from the local Universe. In Tables 2 and 3, the predicted spatial galaxy densities at $z = 0$ are given for absorber density distribution functions fitted to the high-redshift data (Figs. 3 to 5). In the diffeomorphic approach, a spatial density of at least $1.5\,10^{-2}$ large spirals per Mpc is expected at $z = 0$. Assuming disk masses given in Table 1, along with a mass-to-luminosity ratio $m/L_B \approx 2...5$ in solar units (Binney & Merrifield 1998; Gnedin & Ostriker 1992), such number density corresponds to a present luminosity density $\mathcal{L}_B \approx (2...5)\,10^8\,L_{B\odot}\,\mathrm{Mpc}^{-3}$ which is too high by a factor of at least 2 when compared with observations (Binggeli et al. 1988). Taking into account the mass distribution via the galaxy LF we find $\Phi_* \gtrsim 4\,10^{-3}\,\mathrm{Mpc}^{-3}$ for models providing a reasonable fit to the data. This is also about a factor of two larger than the corresponding values for the observed spiral LF (see Sect. 4). Zucca et al. (1997) list the parameters for the total LF from various samples. The most results are consistent with $\Phi_* \approx 2.5\,10^{-3}\,\mathrm{Mpc}^{-3}$. The predicted frequency distribution of HI column densities at $z = 0$ is, at least, a factor of two too large when compared with the observational data derived from HI gas in nearby galaxies (Fig. 6), though the slope of the distributions

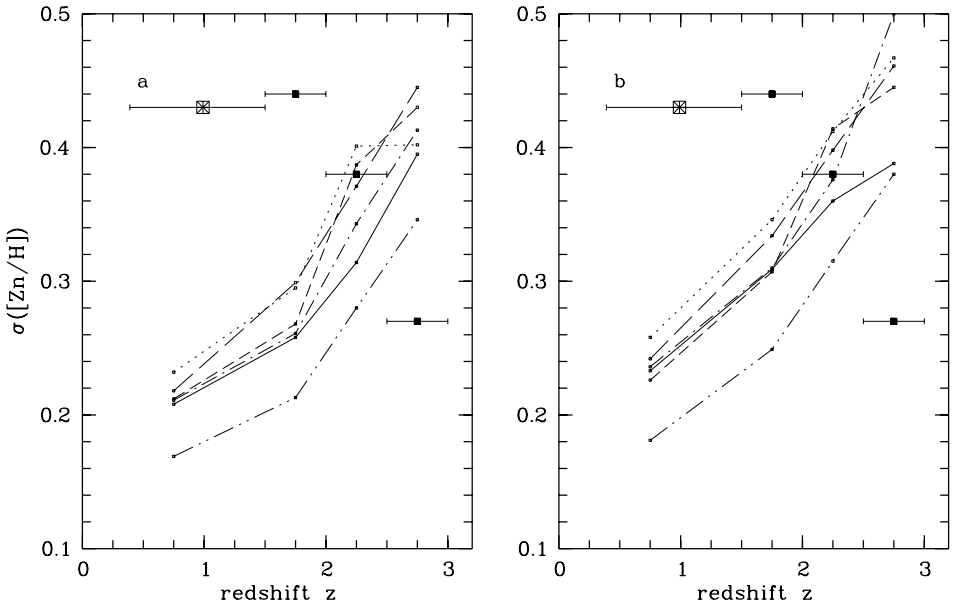

Fig. 12a and b. The standard deviation $\sigma_{[\mathrm{Zn/H}]}$ of dLyα systems with zinc column densities $N(\mathrm{Zn}) \leq 1.4\,10^{13}\,\mathrm{cm}^{-2}$ in binning intervals of z. **a** and **b** as in Fig. 11. For the sake of clearness, the values predicted by a model are interconnected by lines with the same meaning of the style as in the previous figures. The predicted scatters account also for inhomogeneous chemical evolution in the models. The empirical data are the same as in Figs. 7, 8 and 11. The horizontal lines indicate the widths of the binning intervals.

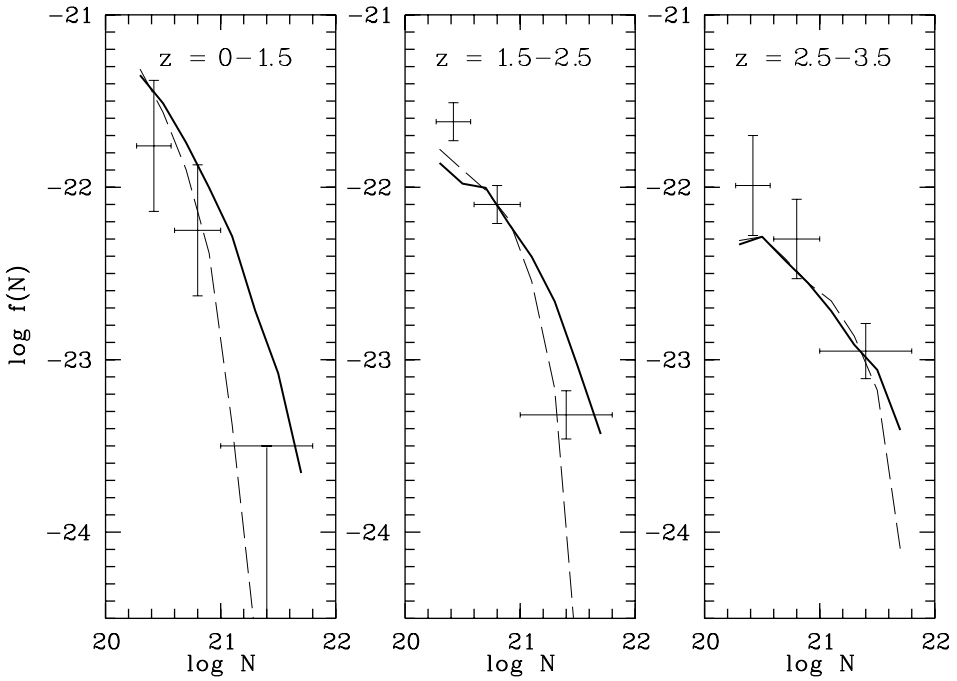

Fig. 13. As Fig. 3, but from MC simulations for model 1 only. The thick, solid curves represent the unbiased case, whereas the dashed curves result when systems with $N(\mathrm{Zn}) > 1.4\,10^{13}\,\mathrm{cm}^{-2}$ are excluded due to dust extinction.

are in good agreement with the observational data. The other way round, it seems that only about half the high-redshift dLyα absorbers is related to the progenitors of large spiral galaxies of the local galaxy population at $z = 0$.

Obviously, the discrepancy would naturally disappear if there exists a population of galaxies which are similar to large spirals in some sense but which are missed in local galaxy surveys. Galaxies of low surface brightness (LSB) are probably good candidates. According to modern disk formation scenarios, LSB disks form naturally in low-mass and/or high angular momentum halos (Dalcanton et al. 1997b; Jimenez et al. 1997; Mo et al. 1998). Indeed, LSB galaxies are found to contribute significantly to the galaxy population in the local Universe (Impey et al. 1988; Irwin et al. 1990; McGaugh 1996; Sprayberry et al. 1997; Dalcanton et al. 1997a), and it has been speculated that current measurements of the galaxy LF may be missing a large fraction of all L_* galaxies due to their low surface brightness (Delcanton et al. 1997b). Mo et al. (1998) have emphasized that the galaxy population associated with damped absorbers should be biased towards such LSB systems because the absorption cross section is strongly weighted towards disks with large size for their mass. LSB galaxies have already been identified with systems associated with dLyα absorption (see e.g., Timmes et al. 1995a; Pettini et al. 1997) and may be the counterparts of low-z dLyα systems not identified in deep imaging studies (Steidel et al. 1997; Rao & Turnshek 1998). If LSB galaxies are unevolved

objects collapsed only at late time (McGaugh & Bothun 1994; Mo et al. 1994; De Blok et al. 1995) they would contribute to the dLyα statistics predominantly in the lowest redshift bin. It is tempting to speculate that LSB galaxies fill the gap between the observed frequency distribution of dLyα column densities and the lower frequency of predicted high-column density systems after the dust extinction bias is taken into account (Fig. 13). The chemical properties of LSB galaxies (see Jimenez et al. 1998) seem to be consistent with such an interpretation. Unfortunately, the evolutionary state of LSB galaxies is not yet fully understood. Jimenez et al. (1998) emphasized that LSB galaxies have similar colours as high surface brightness galaxies; hence, their ages and SFR histories may be similar, too. Furthermore, it has been suspected that the contribution of LSB galaxies to the HI mass density at $z = 0$ is low (Zwaan et al. 1997), and it is not yet clear whether LSB systems really contribute significantly to the galaxy density at L_* (Sprayberry et al. 1997). Thus, there is not yet clear-cut evidence that a substantial fraction of dLyα absorbers is related to LSB galaxies. To summarize, LSB galaxies probably contribute to the sample of dLyα absorption systems, but their rôle for the statistics of absorber galaxies still remains unclear.

For the sake of completeness of the discussion, we refer to another possible solution for the discrepancy between the number density of high redshift dLyα systems and their expected local counterparts. It seems very unlikely that this discrepancy is due to strong density evolution near $z = 0$. However, it may be due to the large scale cosmic structure. It can not be definitively excluded that the galaxy density in the local Universe is lower than the average density, as has been proposed for different reasons earlier (Turner et al. 1992; Bartlett et al. 1995; Zehavi et al. 1998). Results from recent galaxy surveys are not inconsistent with the possibility that the local region is underdense, perhaps by a factor of about 2 (cf. the discussion by Marzke et al. 1998).

8. Conclusions

We have studied in detail models for the viscous evolution of the Galactic disk including secular gas infall. In paper 1, it was shown that such models can reproduce many of the observed properties of the Galactic disk, in particular the exponential stellar density profile, the flat inner rotation curve, the G dwarf metallicity distribution, the oxygen-to-iron element abundance ratio, and the existence of radial abundance gradients. In the present paper, we have used such models to make inferences about the properties of disk galaxies at high redshift. We have confronted the model predictions with constraints derived from observational data on the evolution with redshift of the SFR, the distribution $f(N)$ of the H I column density, and on cosmic chemical evolution. The basic assumptions are that dLyα systems (essentially) represent early evolutionary stages of present day disk galaxies and that the Milky Way disk is representative for such galaxy disks.

We studied models with different descriptions of the SFR and the viscosity: the ΣR-model and the Q-model. The main difference in the properties of the resulting model disk is a flatter gas density profile and a steeper radial abundance gradient in the Q-model. The inferences from the models for high redshifts depend also on the rôle of gas infall. Variations in other model properties (Lin-Pringle parameter β, inclusion of infall-induced radial gas flows, temporary action of a central bar) are of minor importance. We have considered models with two types of infall histories. Slow disk evolution models with strong gas infall are in poor agreement with all observational constraints. Moderate infall models provide a better agreement.

The observed shape of the frequency distribution of H I column densities, $f(N, z)$, of dLyα absorbers is roughly reproduced by the moderate infall ΣR-models, but not for the Q-model. The fit is substantially improved for all models after a mass spectrum of absorber galaxies is accounted for corresponding to the luminosity function of spiral galaxies. The same models provide also a reasonable fit of the redshift-[Zn/H] relation. At intermediate redshifts, the predicted abundance scatter is smaller than the observed one.

The situation is significantly changed after a selection bias due to dust extinction is taken into account. Then, the fit of the redshift-[Zn/H] relation is improved while the predicted abundance scatter at intermediate and low redshifts is further reduced, and the predicted number density of observed high column density absorbers at $z \approx 1$ is too low. Generally, there is an overabundance of alpha elements relative to iron peak elements in the model data at high redshift. The abundance ratio [Si/Fe] predicted by the models strongly disagree with the observations if dust depletion estimates by Vladilo (1998) are adopted. It is tempting to speculate that better agreement between model predictions and observational data can be achieved on the asumption that dLyα absorption systems are associated with various galaxy types. LSB galaxies are good candidates for a substantial fraction dLyα systems.

The approach of the present study may be too simple in several points: First, we have studied only one special type of evolution models for the Galactic disk. Further, we have simulated the effect of the galaxy LF in the context of the HI column density evolution but not in the context of chemical evolution. Various galaxy types have been simulated simply by scaling the mass and gas densities. However, a more realistic approach should consider different SFR histories for different types of spiral galaxies (Kennicutt 1998). For example, early type galaxies must drop out of the statistics when the gas is used up, but this has not yet been taken into account. (The expected effect is a further steepening in $f(N)$ with decreasing z.) Estimating the contribution of LSB galaxies to the statistics of dLyα absorber systems seems to be of particular importance. Finally, effects of gravitational interactions, like gas stripping and merging, have not been considered yet.

Acknowledgements. H.M. is grateful to G. Kauffmann and K. Nomoto for helpful discussions and to M. Pettini for sending re- and preprints. R.T. acknowledges financial support from the Deutsche Forschungsgemeinschaft under grant ME 1350/2-2.

Appendix A: Monte Carlo simulations

We applied Monte Carlo simulations to compute mean element abundances for random distributions of sightlines. A line of sight is charactarized by three parameters: the inclination angle i to the galactic plane, the angle α between the sightline and the direction toward the galactic centre, and the galactocentric distance, R_c, of the point where the sightline crosses the galactic plane. The corresponding probability densities are $f(i) \propto \sin i$, $f(\alpha) = \text{const.}$, and $f(R_c) \propto R_c$ for $i = 0...\pi$, $\alpha = 0...\pi/2$, and $R_c = 0...R_{max}$. The distribution of dLyα systems with redshift is described by $f(z) \propto (1+z)^{1/2}$ (cf. Sect. 4).

Assuming an exponential density distribution perpendicular to the galactic plane the column density $N(\mathrm{X})$ of a chemical element X along the line of sight (i, α, R_c) is given by

$$N(\mathrm{X}) = \int_o^\infty n(\mathrm{X}; s)\, ds = \int_0^\infty n(\mathrm{X}; r)\, e^{-|z(r)|/\lambda} \frac{dr}{\cos i}, \quad \text{(A1)}$$

where s is measured along the sightline, and r is measured along the projection of the sightline onto the galactic plane; z is the distance from the plane; λ is the vertical scale height of the gas. The space density $n(\mathrm{X})$ of elements X can be expressed in terms of the galactic surface density of hydrogen atoms, Σ_H, along with the abundance ratio [X/H]

$$N(\mathrm{X}) = \frac{(\mathrm{X/H})_\odot}{2\,\lambda \cos i} \int_0^\infty \Sigma_\mathrm{H}(R[r])\, 10^{\,[\mathrm{X/H}]}\, e^{-|z(r)|/\lambda}\, dr, \quad \text{(A2)}$$

where Σ_H and [X/H] are given by the model. R and z are given by simple trigonometric relations

$$z = (r - r_c) \tan i, \quad \text{(A3)}$$

$$R = (R_c^2 + (r_c - r)^2 + 2R_c(r_c - r)\cos\alpha)^{1/2}, \quad \text{(A4)}$$

$$r_c = (R_{max}^2 - R_c^2 + (R_c \cos\alpha)^2)^{1/2} - R_c \cos\alpha. \quad \text{(A5)}$$

We adopt $R_{max} = 40\,\mathrm{kpc}$ (i.e., the outer limit in the model calculations) and $\lambda = 0.1\,\mathrm{kpc}$. The results do not depend on the exact value of λ as long as λ is much smaller than the scale length of the gaseous disk.

Column-density weighted mean abundances as defined by Pettini et al. (1997) are computed by the summation over all m sightlines for which the hydrogen column density corresponds to dLyα systems

$$[\langle \mathrm{X/Y} \rangle] = \log S_\mathrm{X} - \log S_\mathrm{Y} \text{ for } N_i(\mathrm{H}) \geq 2\,10^{20}\,\mathrm{cm}^{-2}, \quad \text{(A6)}$$

with

$$S_\mathrm{X} = \sum_{i=1}^{m} \Big[\int_0^\infty \Sigma_\mathrm{H}(R[r])\, 10^{\,[\mathrm{X/H}]}\, e^{-|z(r)|/\lambda}\, dr \Big]_i$$

$$S_\mathrm{Y} = \sum_{i=1}^{m} \Big[\int_0^\infty \Sigma_\mathrm{H}(R[r])\, 10^{\,[\mathrm{Y/H}]}\, e^{-|z(r)|/\lambda}\, dr \Big]_i$$

where $N_i(\mathrm{H})$ is given by Eq. (A.2).

Typically 10^4 sightlines were simulated for the calculation of mean abundance ratios yielding about 10^3 dLyα systems. Dust extinction effects, as discussed in Sect. 6, are easily taken into account by the additional constraint $\log N_i(\mathrm{Zn}) \leq 13.15$.

References

Aragón-Salamanca A., Ellis R.S., O'Brien K.S., 1996, MNRAS 281, 945

Bartlett J.G., Blanchard A., Silk J., Turner M.S., 1995, Sci 267, 980

Bechtold J., Elston R., Yee H.K.C., Ellingson E., Cutri R.M., 1998, In: D'Odorico S., Fontana A., Giallongo E. (eds.) The Young Universe: Galaxy Formation and Evolution at Intermediate and High Redshift. ASP Conf. Ser. 146, p. 241

Binggeli B., Sandage A., Tammann G.A., 1988, ARA&A 26, 509

Binney J., Merrifield M., 1998, Galactic Astronomy. Princeton University Press, Princeton

Black J.H., Chaffee F.H., Foltz C.B., 1987, ApJ 317, 442

Blades C.J., Turnshek D.A., Norman C.A., 1988, In: Blades C.J., Turnshek D.A., Norman C.A. (eds.) QSO Absorption Lines: Probing the Universe. Cambridge University Press, Cambridge

Blumenthal G.R., Faber S.M., Flores R., Primack J.R., 1986, ApJ 391, 27

Brunzendorf J., Meusinger H., 1999, A&A in press

Boissé P., 1995, In: Meylan G. (ed.), QSO Absorption Lines. Springer, Berlin, p. 35

Boissé P., Le Brun V., Bergeron J., Deharveng J.-M., 1998, A&A 333, 841

Brinchmann J., Abraham R., Schade D., et al., 1998, ApJ 499, 112

Casoli F., Sauty S., Gerin M., et al., 1998, A&A 331, 451

Cassé M., Olive K.A., Vangioni-Flam E., Audouze J., 1998, New astronomy 3, 259

Chaffee F.H., Black J.H., Foltz C.B., 1988, ApJ 335, 584

Chen H.-W., Lanzetta K.M., Webb J.K., Barcons X., 1998, ApJ 498, 77

Clarke C., 1989, MNRAS 238, 283

Connolly A.J., Szalay A.S., Dickinson M., Subbarao M.U., Brunner R.J., 1997, ApJ 486, L11

Courthau S., De Jong R.S., Broeils A.H., 1996, ApJ 457, L73

Dalcanton J.J., Spergel D.N., Gunn J.E., Schmidt M., Schneider D.P., 1997a, AJ 114, 635

Dalcanton J.J., Spergel D.N., Summers F.J., 1997b, ApJ 482, 659

De Blok W.J.G., van der Hulst J.M., Bothun G.D., 1995, MNRAS 274, 235

de la Varga A., Reimers D., 1998, In: Petitjean P., Charlot S. (eds.) Structure and Evolution of the Intergalactic Medium from QSO Absorption Line Systems. Editions Frontiéres, Paris, 456

Djorgovski S.G., Pahre M.A., Bechtold J., Elston R., 1996, Nat 382, 234

D'Odorico S., Fontana A., Giallongo E., 1998, In: D'Odorico S., Fontana A., Giallongo E. (eds.) The Young Universe: Galaxy Formation and Evolution at Intermediate and High Redshift. ASP Conf. Ser. 146

Duquennoy A., Mayor M., 1991, A&A 248, 485

Ellis R.S., Colless M., Broadhurst T., Heyl J., Glazebrook K., 1996, MNRAS 280, 235

Fall M.S., Pei Y.C., McMahon R.G., 1989, ApJ 341, L5

Fall S.M., Pei Y.C., 1993, ApJ 402, 479

Fan X.-M., Tytler D., 1994, ApJS 94, 17

Foltz C.B., Chaffee F.H., Wolfe A.M., 1988, ApJ 335, 35

Fynbo J.U., Møller P., Warren S.J., 1999, ESO preprint 1326

Gallego J., Zamorano J., García-Dabó C.E., Aragón-Salamanca A., Guzmán R., 1998, In: D'Odorico S., Fontana A., Giallongo E. (eds.) The Young Universe: Galaxy Formation and Evolution at Intermediate and High Redshift. ASP Conf. Ser. 146, p. 235

Ge J., Bechtold J., 1997, ApJ 477, L73

Gnedin N.Y., Ostriker J.P., 1992, ApJ 400, 1

Green R.F., York D., Huang K., et al., 1995, In: Meylan G. (ed.) QSO Absorption Lines. Springer, Berlin, p. 85
Greggio L., Renzini A., 1983, A&A 118, 217
Haehnelt M.G., Steinmetz M., Rauch M., 1998, ApJ 495, 647
Hewett P.C., Foltz C.B., Chaffee F.H., 1995, AJ 109, 1498
Heyl J., Colless M., Ellis R.S., Broadhurst T., 1997, MNRAS 285, 613
Impey C., Bothun G., Malin D., 1988, ApJ 330, 634
Irwin M.J., Davies J.I., Disney M.J., Phillips S., 1990, MNRAS 245, 289
Jedamzik K., Prochaska J.X., 1998, MNRAS 296, 430
Jimenez R., Heavens A.F., Hawkins M.R.S., Padoan P., 1997, MNRAS 292, L5
Jimenez R., Padoan P., Matteucci F., Heavens A.F., 1998, MNRAS 299, 123
Kauffmann G., 1996, MNRAS 281, 475
Kennicutt R.C., Tamblyn P., Congdon C.W., 1994, ApJ 435, 22
Kennicutt R.C., 1998, ARA&A 36, 189
Khersonsky V.K., Turnshek D.A., 1996, ApJ 471, 657
Kroupa P., Tout C.A., Gilmore G., 1993, MNRAS 262, 545
Lanzetta K.M., Wolfe A.M., Turnshek D.A., et al., 1991, ApJS 77, 1
Lanzetta K.M., Wolfe A.M., Turnshek D.A., 1995, ApJ 440, 435
Lanzetta K.M., Wolfe A.M.,Altan H., Barcons X, Chen H.-W., 1997, AJ 114, 1337
Larson R.B., 1972, Nature Phys. Sci. 236, 7
Le Brun V., Bergeron J., Boissé P., Deharveng J.M., 1997, A&A 321, 733
Le Brun V., Bergeron J., 1998, A&A 332, 814
Ledoux C., Petitjean P., Bergeron J., Wampler E.J., Srianand R., 1998, A&A 337, 51
Leibundgut B., Robertson G., 1998, MNRAS 303, 711
Levshakov S.A., Chaffee F.H., Foltz C.B., Black J.H., 1992, A&A 262, 385
Lilly S.J., Tresse L., Hammer F., Crampton D., LeFevre O., 1995, ApJ 455, 108
Lilly S.J., LeFevre O., Hammer F., Crampton D., 1996, ApJ 460, L1
Lin D.N.C., Pringle J.E., 1987a, ApJ 320, L87
Lin D.N.C., Pringle J.E., 1987b, MNRAS 225, 607
Lin H., Yee H.K.C., Carlberg R.G., Ellington E., 1997, ApJ 475, 494
Lu L., Sargent W.L.W., Barlow T.A., Churchill C.W., Vogt S.S., 1996, ApJS 107, 475
Luck R.E., Bond H.E., 1985, ApJ 292, 559
Lynden-Bell D., 1975, Vistas in Astronomy 19, 299
Madau P., Ferguson H.C., Dickinson M.E., et al., 1996, MNRAS 283, 1388
Madau P., Pozzetti L., Dickinson M., 1998, ApJ 498, 106
Malaney R.A., Chaboyer B., 1996, ApJ 462, 57
Mannucci F., Thompson D., Beckwith V.W., Williger G.M., 1998, ApJ 501, L11
Marzke R.O., Geller M.J., Huchra J.P., Corwin H.G., 1994, AJ 108, 2
Marzke R.O., da Costa L.N., Pellegrini P.S., Willmer N.A., Geller M.J., 1998, ApJ 503, 617
Matteucci F., Greggio L., 1986, A&A 154, 279
Matteucci F., Francois P., 1989, MNRAS 239, 885
Matteucci F., Molaro P., Vladilo G., 1997, A&A 321, 45
McGaugh S.S., 1996, MNRAS 280, 337
McGaugh S.S., Bothun G.D., 1994, AJ 107, 530
Meyer D.M., York D.G., 1987, ApJ 319, L45
Meyer D.M., Welty D.E., York D.G., 1989, ApJ 343, L37
Meyer D.M., Roth K.C., 1990, ApJ 363, 57
Meyer D.M., York D.G., 1992, ApJ 399, L121
Michalitsianos A.G., Dolan J.F., Kazanas D., et al., 1997, ApJ 474, 598
Mo H.J., McGaugh S.S., Bothun G.D., 1994, MNRAS 267, 129
Mo H.J., Mao S., White S.D.M., 1998, MNRAS 295, 319
Molaro P., D'Odorico S., Fontana A., Savaglio S., Vladilo G., 1996, A&A 308, 1
Molaro P., Centurión M., Vladilo G., 1998, MNRAS 293, 37
Møller P., Warren S.J., 1993, A&A 270, 45
Møller P., Warren S.J., Fynbo J., 1998, A&A 330,19
Nissen P.E., Schuster W.J., 1997, A&A 326, 751
Nomoto K., Hashimoto M., Tsujimoto T., et al., 1997a, Nucl. Phys. A, 616, 79
Nomoto K., Iwamoto K., Nakasato N., et al., 1997b, Nucl. Phys. A, 621, 467
Olivier S.O., Blumenthal G.R., Primack J.R., 1991, MNRAS 252, 102
Pagel B.E.J., Patchett B.E., 1975, MNRAS 172, 13
Peebles P.J.E., 1993, Principles of Physical Cosmology. Princeton University Press, Princeton
Pei Y.C., Fall S.M., Bechtold J., 1991, ApJ 378, 6
Pei Y.C., Fall S.M., 1995, ApJ 454, 69
Pettini M., Boksenberg A., Hunstead R.W., 1990, ApJ 348, 48
Pettini M., Smith L.J., Hunstead R.W., King D.L., 1994, ApJ 426, 79
Pettini M., Lipman K., Hunstead R.W., 1995a , ApJ 451, 100
Pettini M., Hunstead R.W., King D.L., Smith L.J., 1995b, In: Meylan G. (ed.) QSO Absorption Lines. Springer, Berlin, p. 55
Pettini M., Smith L.J., King D.L., Hunstead R.W., 1997, ApJ 486, 665
Pettini M., Ellison S.L., Steidel C.C., Bowen D.V., 1999a, ApJ 510, 576
Pettini M., Ellison S.L., Steidel C.C., Shapley A.E., Bowen D.V., 1999b, preprint
Pilyugin L.S., Edmunds M.G., 1997, A&A 313, 783
Prantzos N., Aubert O., 1995, A&A 302, 69
Pringle J.E., 1981, ARA&A 19, 135
Prochaska J.X., Wolfe A.M., 1997, ApJ 474, 140
Rao S.M., Briggs F., 1993, ApJ 419, 515
Rao S.M., Turnshek D.A., 1998, ApJ 500, L115
Rauch M., Carswell R.F., Robertson J.G., Shaver P.A., Webb J.K., 1990, MNRAS 242, 698
Sandage A., Binggeli B., Tammann G.A., 1985, AJ 90, 1759
Sawicki M.J., Lin H., Yee H.K.C., 1997, AJ 110, 68
Silk J., Norman C., 1981, ApJ 247, 59
Sneden C., Gratton R., Crocker D.A., 1991, A&A 246, 354
Sommer-Larsen J., Yoshii Y., 1989, MNRAS 238, 133
Sommer-Larsen J., Yoshii Y., 1990, MNRAS 243, 468
Sprayberry D., Impey C., Irwin M.J., Bothun G.D., 1997, ApJ 481, 104
Srianand R., Petitjean P., 1998, A&A 335, 33
Steidel C.C., 1995, In: Meylan G. (ed.) QSO absorption lines. Springer, Berlin, p. 139
Steidel C.C., Bowen D.V., Blades J.C., Dickinson M., 1995, ApJ 440, L45
Steidel C.C., Dickinson M., Meyer D.M., Adelberger K.L., Sembach K.R., 1997, ApJ 480, 568
Storrie-Lombardi L.J., McMahon R.G., Irwin M.J., 1996, MNRAS 283, L79
Tammann G.A., 1986, In: Kunth D., Thuan T.X., Tran Than Van J. (eds.) Star-forming dwarf galaxies and related objects. Editions Frontiéres, Gif-sur-Yvette, p. 41
Thon R., Meusinger H., 1998, A&A 338, 413 (paper 1)
Timmes F.X., Lauroesch J.T., Truran J.W., 1995a, ApJ 451, 468
Timmes F.X., Woosley S.E., Weaver T.A., 1995b, ApJS 98, 617
Tinsley B.M., 1980, Fund. Cosmic Phys. 5, 287
Tsujimoto T., Yoshii Y., Nomoto K., Shigeyama T., 1995, A&A 302, 945

Turner E.L., Cen R., Ostriker J.P., 1992, ApJ 103, 1427
Tyson N.D., 1988, ApJ 329, L57
van den Hoek L.B., de Jong T., 1997, A&A 318, 231
Vladilo G., 1998, ApJ 493, 583
Wang B., Silk J., 1994, ApJ 427, 759
Weymann R.J., Carswell R.F., Smith M.G., 1981, ARA&A 19, 41
White S.D.M., Rees M.J., 1978, MNRAS 183, 341
Wolfe A.M., 1988, In: Blades J.C., Turnshek D.A., Norman C.A. (eds.) QSO Absorption Lines: Probing the Universe. Cambridge University Press, Cambridge, p. 297
Wolfe A.M., 1995, In: Meylan G. (ed.) QSO Absorption Lines. Springer, Berlin, p. 13
Wolfe A.M., Turnshek D.A., Smith H.E., Cohen R.D., 1986, ApJS 61, 249
Wolfe A.M., Lanzetta K.M., Foltz C.B., Chaffee F.H., 1995, ApJ 454, 698
Wolfe A.M., Prochaska J.X., 1998, ApJ 494, L15
Woosley S.E., Weaver T.A., 1995, ApJS 101, 181
Wyse R.F.G., Gilmore G., 1993, In: Smith G.H., Brodie J.P. (eds.) The Globular Cluster-Galaxy Connection. ASP Conf. Ser. 48, p. 727
Yoshii Y., Sommer-Larsen J., 1989, MNRAS 236, 779
York D.G., 1988, In: Blades J.C., Turnshek D.A., Norman C.A. (eds.) QSO Absorption Lines: Probing the Universe. Cambridge University Press, Cambridge, p. 227
Zehavi I., Riess A.G., Kirshner R.P., Dekel A., 1998, ApJ 503, 483
Zucca E., Zamorani G., Vettolani G., et al., 1997, A&A 326, 477
Zwaan M.A., Briggs F.H., Sprayberry D., Sorar E., 1997, ApJ 490, 173